

Resonant transducers for a spherical GW antenna

J. Alberto Lobo and M. Angeles Serrano

*Departament de Física Fonamental
Universitat de Barcelona, Spain.*

(3 June 1997)

(Revised September 4, 2018)

Apart from omnidirectional, a solid elastic sphere is a multimode and multifrequency device for the detection of Gravitational Waves (GW). Motion sensing in a spherical GW detector thus naturally requires a multiple set of transducers attached to its surface at suitable locations. If these transducers are of the resonant type then their motion couples to that of the sphere, and the *joint dynamics* of the system has to be properly understood before reliable conclusions can be drawn from its readout. In this paper we address the problem of the coupled motion of a solid elastic sphere and a set of resonators attached to its surface in full theoretical rigor. A remarkably elegant and powerful scheme is seen to emerge from the general equations which shows with unprecedented precision how coupling takes place as a series function of the small “coupling constant” η , the ratio of the resonators’ average mass to the sphere’s mass. We reassess in the new light the response of the highly symmetric truncated icosahedron layout (the *TIGA*), and also present a new proposal (the pentagonal hexacontahedron, or *PHC*), which has less symmetry but requires only 5 rather than 6 transducers. We finally address the question of how the system characteristics are affected by slight departures from perfect spherical symmetry and identity of resonators, and find it to be quite *robust* against such small failures. In particular, we recover with fully satisfactory accuracy the reported experimental frequencies of the reduced scale prototype detector constructed and tested at *LSU*.

04.80.Nn, 95.55.Ym

I. INTRODUCTION

The idea of using a solid elastic sphere as a gravitational wave (GW) antenna is almost as old as that of using cylindrical bars: as far back as 1971 Forward published a paper [1] in which he assessed some of the potentialities offered by a spherical solid for that purpose. It was however Weber’s ongoing philosophy and practice of using bars which eventually prevailed and developed up to the present date, with the highly sophisticated and sensitive ultracryogenic systems currently in operation —see [2] and [3] for rather detailed reviews and bibliography. With few exceptions [4,5], spherical detectors fell into oblivion for years, but interest in them strongly re-emerged in the early 1990’s, and an important number of research articles have been published since which address a wide variety of problems in GW spherical detector science. At the same time, international collaboration has intensified, and prospects for the actual construction of large spherical GW observatories (in the range of ~ 100 tons) are being currently considered in several countries [6], even in a variant *hollow* shape [7].

A spherical antenna is obviously omnidirectional but, most important, it is also a natural *multimode* device, i.e., when suitably monitored, it can generate information on the GW amplitudes and incidence direction [5,8], a capability which possesses no other individual GW detector, whether resonant or interferometric. Furthermore, a spherical antenna could also reveal the eventual existence of *monopole* gravitational radiation, or set thresholds on it [9]. The theoretical explanation of these facts is to be found in the unique matching between the GW amplitude structure and that of the sphere oscillation eigenmodes: a general *metric* GW generates a *tidal* field of forces in an elastic body which is given in terms of the “electric” components $R_{0i0j}(t)$ of the Riemann tensor at its centre of mass by the following formula [10]:

$$\mathbf{f}_{\text{GW}}(\mathbf{x}, t) = \sum_{\substack{l=0 \text{ and } 2 \\ m=-l, \dots, l}} \mathbf{f}^{(lm)}(\mathbf{x}) g^{(lm)}(t) \quad (1.1)$$

where $\mathbf{f}^{(lm)}(\mathbf{x})$ are pure “tidal form factors”, while $g^{(lm)}(t)$ are suitable linear combinations of the Riemann tensor components $R_{0i0j}(t)$ which carry all the *dynamical* information on the GW’s monopole ($l=0$) and quadrupole ($l=2$) amplitudes.

On the other hand, a free elastic sphere has two families of oscillation eigenmodes, so called *toroidal* and *spheroidal* modes, and modes within either family group into ascending series of l -pole harmonics, each of whose frequencies is

$(2l+1)$ -fold degenerate —see [10] for full details. It so happens that *only* monopole and/or quadrupole spheroidal modes can possibly be excited by an incoming *metric* GW [11], and their GW driven amplitudes are directly proportional to the wave amplitudes $g^{(lm)}(t)$ of equation (1.1). It is this very fact which makes of the spherical detector such a natural one for GW observations [10]. In addition, a spherical antenna has a significantly higher absorption *cross section* than a cylinder of like fundamental frequency, and also presents good sensitivity at the *second* quadrupole harmonic [12].

But GW excitations are *extremely weak* [13], and so a suitable readout system must be *added* to the sphere in order to monitor its motions and quantitatively assess their magnitude and physical significance. In cylindrical bars, current state of the art technology is based upon *resonant transducers* [14–18]. A resonant transducer consists in a small (compared to the cylinder) mechanical device possessing a resonance frequency accurately tuned to that of the cylinder. This *frequency matching* causes back-and-forth *resonant energy transfer* between the two bodies (bar and resonator), which results in turn in *amplified* oscillations of the smaller resonator. The *energy* amplification factor is $M_{\text{resonator}}/M_{\text{bar}}$, hence the *amplitude* amplification is the *square root* of this mass ratio. Pre-electronics mechanical amplification is highly desirable, given the exceedingly small magnitude of any expected GW signals arriving in the observatory.

The philosophy of using resonators for motion sensing is directly transplantable to a spherical detector, but a *multiple* set rather than a single resonator is required if its potential capabilities as a multimode system are to be exploited to satisfaction. The practical feasibility of a multiple transducer readout system has been recently demonstrated *experimentally* with encouraging success by S. Merkowitz and W. Johnson at *LSU*, where a 740 kg prototype, milled in the shape of a *truncated icosahedron*, and endowed with a highly symmetric set of 6 resonators, was put to test [19–22]. Their authors call this system *TIGA*, an acronym for *Truncated Icosahedron Gravitational Antenna*.

One of the pillars of the success of this prototype experiment has been M&J’s ability to give an adequate *theoretical interpretation* of their experimental results. M&J’s model of the coupled dynamics of sphere and resonators is based upon the hypothesis that *only* quadrupole excitations of the sphere’s modes need to be considered in a GW detector, *even if* resonators are attached to the sphere’s surface. This extrapolation of a result which, as we have just mentioned, does hold exactly for a *free* sphere, produces remarkably accurate predictions of the *coupled* system behaviour, too, even though interactions of the resonator set with the other, non-quadrupole sphere’s modes are neglected from the beginning. This is a strong indication that such neglected effects are *second order* for the accuracy of the experimental data.

But what does “second order” precisely mean? The answer to such question requires the construction of a more elaborate model, which should be suitable to address in a systematic way any dynamical effects, and to *quantitatively* assess their real importance. The interest of a more sophisticated analysis is to understand and make clear the nature of a given approximation scheme, as well as to enable further refinement of it, if eventually required; its practical relevance is related to the reasonable expectation that future real spherical GW detectors will make use of extremely precise measurement techniques, likely to be rather demanding as regards accurate theoretical modeling of the system.

The purpose and motivation of this paper is to present and develop such a more refined mathematical model. We address the the problem of the joint dynamics of a spherical elastic solid endowed with a set of radial resonators, with as few as possible unwarranted hypotheses, and with the objective to determine the system response to any interesting signals, whether GWs or calibration inputs, with unlimited mathematical precision. As we shall see, the model confirms and generalises that of Merkowitz and Johnson [19,22] in the sense of making precise its actual range of applicability. More specifically, we shall see that the solution to our general equations of motion can be written as a *perturbative* series expansion in ascending powers of the small *coupling constant* $\eta^{1/2}$ ($\eta \equiv M_{\text{resonator}}/M_{\text{sphere}}$), whose *lowest order* terms exactly correspond to Merkowitz and Johnson’s model. This is a key result, showing that the above alluded “second order” effects are precisely order η effects, or that M&J’s model is accurate up to relative errors of this order.

Beyond this, though, a remarkably elegant, simple, and powerful algebraic scheme will be seen to emerge from the theory, which neatly displays the basic structure of the system for *completely general* resonator distributions over the sphere’s surface. Based on the resulting equations we already advanced in references [23,24] a genuine transducer layout with 5 rather than 6 resonators, which we propose to call *PHC* (for *pentagonal hexacontahedron*, the shape of the underlying polyhedron), and which we shall also consider here in parallel with the more symmetric *TIGA* of Merkowitz and Johnson.

The paper will be structured as follows. Section 2 is devoted to present the main hypotheses of the model and the general equations, whose reduction to a tractable set is described in detail in section 3. Sections 4 and 5 contain a number of general, signal-independent results which apply to an idealised system of perfect sphere and resonators; they constitute the foundations for the analysis of more realistic instances, where one (or more) of the idealised hypotheses partly fails. The system response to an incoming GW is then addressed in section 6, where a complete study of quadrupole *and* monopole radiation sensing is presented for arbitrary transducer layouts. Still within the section, we apply our general results to the important examples of *TIGA* and *PHC*. Section 7 addresses the problem

of the system response to a simple *calibration* signal, an impulsive hammer stroke, and in section 8 we assess the consequences of system defects relative to the idealised perfection assumed that far; more specifically, we consider failures in spherical symmetry and identity of resonator properties, and tolerances in resonator location. In this section we also put to test our model's predictions by confronting them with the reported experimental data obtained in the *TIGA* prototype experiment [21], and see that agreement between both (theory and experiment) is fully satisfactory in the given theoretical and experimental conditions. The paper closes in section 9 with a summary of conclusions.

II. GENERAL EQUATIONS

With minor improvements, we shall use the notation of references [10] and [23], some of which is now briefly recalled. We consider a solid sphere of mass \mathcal{M} , radius R , (uniform) density ϱ , and elastic Lamé coefficients [25] λ and μ , endowed with a set of J resonators of masses M_a and resonance frequencies Ω_a ($a = 1, \dots, J$), respectively. We shall model the latter as *point masses* attached to one end of a linear spring, whose other end is rigidly linked to the sphere at locations \mathbf{x}_a —see Figure 1. The system degrees of freedom are given by the *field* of elastic displacements $\mathbf{u}(\mathbf{x}, t)$ of the sphere plus the *discrete* set of resonator spring deformations $z_a(t)$; equations of motion need to be written down for them, of course, and this is our next concern in this section.

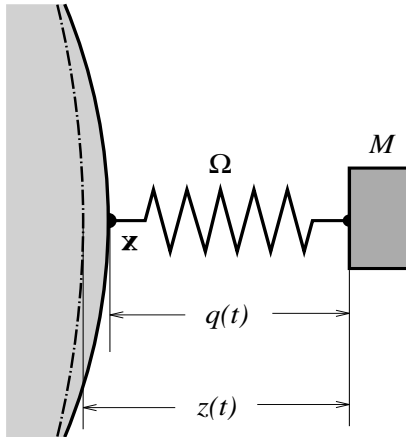


FIG. 1. Schematic diagramme of the coupling model between a solid sphere and a resonator. The notation is that in the text, but subindices have been dropped for clarity. The dashed-dotted arc line on the left indicates the position of the *undeformed* sphere's surface, and the solid arc its *actual* position.

We shall assume that the resonators only move radially, and also that Classical Elasticity theory [25] is sufficiently accurate for our purposes¹. In these circumstances we have [23]

$$\varrho \frac{\partial^2 \mathbf{u}}{\partial t^2} = \mu \nabla^2 \mathbf{u} + (\lambda + \mu) \nabla(\nabla \cdot \mathbf{u}) + \mathbf{f}(\mathbf{x}, t) \quad (2.1a)$$

$$\ddot{z}_a(t) = -\Omega_a^2 [z_a(t) - u_a(t)] + \xi_a(t), \quad a = 1, \dots, J \quad (2.1b)$$

where $\mathbf{n}_a \equiv \mathbf{x}_a/R$ is the outward pointing normal at the the a -th resonator's attachment point, and

$$u_a(t) \equiv \mathbf{n}_a \cdot \mathbf{u}(\mathbf{x}_a, t), \quad a = 1, \dots, J \quad (2.2)$$

is the *radial* deformation of the sphere's surface at \mathbf{x}_a . A dot ($\dot{}$) is an abbreviation for time derivative. The term in square brackets in (2.1b) is thus the spring deformation $-q(t)$ in Figure 1.

¹ We clearly do not expect relativistic motions in extremely small displacements at typical frequencies in the range of 1 kHz.

$\mathbf{f}(\mathbf{x}, t)$ in the rhs of (2.1a) contains the *density* of all *non-internal* forces acting on the sphere, which we expediently split into a component due the resonators' *back action* and an external action *proper*, which can be a GW signal, a calibration signal, etc. Thus

$$\mathbf{f}(\mathbf{x}, t) = \mathbf{f}_{\text{resonators}}(\mathbf{x}, t) + \mathbf{f}_{\text{external}}(\mathbf{x}, t) \quad (2.3)$$

Finally, $\xi_a(t)$ in the rhs of (2.1b) is the force per unit mass (acceleration) acting on the a -th resonator due to *external* agents.

Since we are making the hypothesis that the resonators are point masses the following holds:

$$\mathbf{f}_{\text{resonators}}(\mathbf{x}, t) = \sum_{a=1}^J M_a \Omega_a^2 \delta^{(3)}(\mathbf{x} - \mathbf{x}_a) [z_a(t) - u_a(t)] \mathbf{n}_a \quad (2.4)$$

where $\delta^{(3)}$ is the three dimensional Dirac density function.

The *external* forces we shall be considering in this paper will be *gravitational wave* signals (of course!) and a simple calibration signal, a perpendicular *hammer stroke*. GW driving terms, we recall from (1.1), can be written

$$\mathbf{f}_{\text{GW}}(\mathbf{x}, t) = \mathbf{f}^{(00)}(\mathbf{x}) g^{(00)}(t) + \sum_{m=-2}^2 \mathbf{f}^{(2m)}(\mathbf{x}) g^{(2m)}(t) \quad (2.5)$$

for a general *metric* wave —see [10] for explicit formulas and technical details. While the spatial coefficients $\mathbf{f}^{(lm)}(\mathbf{x})$ are pure *form factors* associated to the *tidal* character of a GW excitation, it is the time dependent factors $g^{(lm)}(t)$ which carry the specific information on the incoming GW. The purpose of a GW detector is to determine the latter coefficients on the basis of suitable measurements.

If a GW sweeps the observatory then the resonators themselves will also be affected, of course. They will be driven, relative to the sphere's centre, by a tidal acceleration which, since they only move radially, is given by

$$\xi_a^{\text{GW}}(t) = c^2 R_{0i0j}(t) x_{a,i} n_{a,j} , \quad a = 1, \dots, J \quad (2.6)$$

where $R_{0i0j}(t)$ are the “electric” components of the GW Riemann tensor at the centre of the sphere, and R is the sphere's radius so that, clearly, $\mathbf{x}_a = R\mathbf{n}_a$. It may now be recalled from reference [10] that

$$c^2 R_{0i0j}(t) = \sum_{\substack{l=0 \text{ and } 2 \\ m=-l, \dots, l}} E_{ij}^{(lm)} g^{(lm)}(t) \quad (2.7)$$

where $E_{ij}^{(lm)}$ is a set of 6 (constant) symmetric matrices which verify²

$$E_{ij}^{(lm)} n_i n_j = Y_{lm}(\mathbf{n}) , \quad l = 0, 2 , \quad m = -l, \dots, l \quad (2.8)$$

Finally thus:

$$\xi_a^{\text{GW}}(t) = R \sum_{\substack{l=0 \text{ and } 2 \\ m=-l, \dots, l}} Y_{lm}(\mathbf{n}_a) g^{(lm)}(t) , \quad a = 1, \dots, J \quad (2.9)$$

We shall also be eventually considering in this paper the response of the system to a particular *calibration* signal, consisting in a hammer stroke with intensity \mathbf{f}_0 , delivered perpendicularly to the sphere's surface at point \mathbf{x}_0 :

$$\mathbf{f}_{\text{stroke}}(\mathbf{x}, t) = \mathbf{f}_0 \delta^{(3)}(\mathbf{x} - \mathbf{x}_0) \delta(t) \quad (2.10)$$

which we have modeled as an impulsive force in both space and time variables. Unlike GW tides, a hammer stroke will be applied on the sphere's surface, so it may have no *direct* effect on the resonators. In other words,

$$\xi_a^{\text{stroke}}(t) = 0 , \quad a = 1, \dots, J \quad (2.11)$$

² $Y_{lm}(\mathbf{n})$ are spherical harmonics [26].

Our fundamental equations thus read

$$\varrho \frac{\partial^2 \mathbf{u}}{\partial t^2} = \mu \nabla^2 \mathbf{u} + (\lambda + \mu) \nabla(\nabla \cdot \mathbf{u}) + \sum_{b=1}^J M_b \Omega_b^2 \delta^{(3)}(\mathbf{x} - \mathbf{x}_b) [z_b(t) - u_b(t)] \mathbf{n}_b + \mathbf{f}_{\text{external}}(\mathbf{x}, t) \quad (2.12a)$$

$$\ddot{z}_a(t) = -\Omega_a^2 [z_a(t) - u_a(t)] + \xi_a(t), \quad a = 1, \dots, J \quad (2.12b)$$

where $\mathbf{f}_{\text{external}}(\mathbf{x}, t)$ will be given by either (2.5) or (2.10), as the case may be. Likewise, $\xi_a(t)$ will be given by (2.9) or (2.11), respectively. The remainder of this paper will be concerned with finding solutions to the system of coupled differential equations (2.12), and with their meaning and consequences.

III. GREEN FUNCTION FORMALISM

An elegant and powerful method to solve equations (2.12) is the Green function formalism. It so happens that, in all instances of our concern here, the force density $\mathbf{f}(\mathbf{x}, t)$ of equation (2.3) is of the *separable type*, i.e., it can be written as a sum of products of a function of the space variables \mathbf{x} times a function of the time variable t . Direct inspection of equations (2.4)-(2.10) readily shows that this is *always* the case. We thus have, generically,

$$\mathbf{f}(\mathbf{x}, t) = \sum_{\alpha} \mathbf{f}^{(\alpha)}(\mathbf{x}) g^{(\alpha)}(t) \quad (3.1)$$

where α is a suitable label. We recall from reference [10] that, in such circumstances, a formal solution can be written down for equation (2.1a) in terms of a *Green function integral*, whereby the following orthogonal series expansion obtains:

$$\mathbf{u}(\mathbf{x}, t) = \sum_{\alpha} \sum_N \omega_N^{-1} f_N^{(\alpha)} \mathbf{u}_N(\mathbf{x}) g_N^{(\alpha)}(t) \quad (3.2)$$

where

$$f_N^{(\alpha)} \equiv \frac{1}{\mathcal{M}} \int_{\text{Sphere}} \mathbf{u}_N^*(\mathbf{x}) \cdot \mathbf{f}^{(\alpha)}(\mathbf{x}) d^3x \quad (3.3a)$$

$$g_N^{(\alpha)}(t) \equiv \int_0^t g^{(\alpha)}(t') \sin \omega_N(t - t') dt' \quad (3.3b)$$

Here, ω_N and $\mathbf{u}_N(\mathbf{x})$ are the eigenfrequencies and associated normalised wavefunctions of the free sphere —see again [10] for a comprehensive characterisation. Also, N is an abbreviation for a multiple index $\{nlm\}$. We quote the result of a few explicit calculations which will be useful later on:

$$f_{\text{resonators}, N}^{(a)} = \frac{M_a}{\mathcal{M}} \Omega_a^2 \mathbf{n}_a \cdot \mathbf{u}_N^*(\mathbf{x}_a), \quad a = 1, \dots, J \quad (3.4a)$$

$$f_{\text{GW}, N}^{(l'm')} = a_{nl} \delta_{ll'} \delta_{mm'} \quad , \quad N \equiv \{nlm\}, \quad l' = 0, 2, \quad m' = -l', \dots, l' \quad (3.4b)$$

$$f_{\text{stroke}, N} = \mathcal{M}^{-1} \mathbf{f}_0 \cdot \mathbf{u}_N^*(\mathbf{x}_0) \quad (3.4c)$$

where the coefficients a_{nl} in (3.4b) are overlapping integrals of $\mathbf{f}^{(lm)}(\mathbf{x})$ across the volume of the sphere [27], and

$$g_{\text{resonators}, N}^{(a)}(t) = \int_0^t [z_a(t') - u_a(t')] \sin \omega_N(t - t') dt' \quad , \quad a = 1, \dots, J \quad (3.5a)$$

$$g_{\text{GW}, N}^{(lm)}(t) = \int_0^t g^{(lm)}(t') \sin \omega_N(t - t') dt' \quad (3.5b)$$

$$g_{\text{stroke}, N}(t) = \sin \omega_N t \quad (3.5c)$$

These expressions can now be substituted into equation (3.2) to obtain the following equivalent set of equations of motion:

$$\mathbf{u}(\mathbf{x}, t) = \sum_N \omega_N^{-1} \mathbf{u}_N(\mathbf{x}) \left\{ \sum_{b=1}^J \frac{M_b}{\mathcal{M}} \Omega_b^2 [\mathbf{n}_b \cdot \mathbf{u}_N^*(\mathbf{x}_b)] g_{\text{resonators}, N}^{(b)}(t) + \sum_{\alpha} f_{\text{external}, N}^{(\alpha)} g_{\text{external}, N}^{(\alpha)}(t) \right\} \quad (3.6a)$$

$$\ddot{z}_a(t) = -\Omega_a^2 [z_a(t) - u_a(t)] + \xi_a(t), \quad a = 1, \dots, J \quad (3.6b)$$

We now specify $\mathbf{x} = \mathbf{x}_a$ in (3.6a) and multiply both sides of the equation by \mathbf{n}_a , thus finding

$$u_a(t) = u_a^{\text{external}}(t) + \sum_{b=1}^J \eta_b \int_0^t K_{ab}(t-t') [z_b(t') - u_b(t')] dt' \quad (3.7a)$$

$$\ddot{z}_a(t) = -\Omega_a^2 [z_a(t) - u_a(t)] + \xi_a(t), \quad a = 1, \dots, J \quad (3.7b)$$

where $u_a^{\text{external}}(t) \equiv \mathbf{n}_a \cdot \mathbf{u}^{\text{external}}(\mathbf{x}_a, t)$, and

$$\mathbf{u}^{\text{external}}(\mathbf{x}, t) = \sum_{\alpha} \sum_N \omega_N^{-1} f_{\text{external}, N}^{(\alpha)} \mathbf{u}_N(\mathbf{x}) g_{\text{external}, N}^{(\alpha)}(t) \quad (3.8)$$

is the sphere's response to an *external force in the absence of resonators*. The form of (3.8) is given in reference [10] for a generic metric GW signal and for a hammer stroke. The *kernel matrix* $K_{ab}(t)$ in (3.7b) is the following weighted sum of diadic products of wavefunctions:

$$K_{ab}(t) = \Omega_b^2 \sum_N \omega_N^{-1} [\mathbf{n}_b \cdot \mathbf{u}_N^*(\mathbf{x}_b)] [\mathbf{n}_a \cdot \mathbf{u}_N(\mathbf{x}_a)] \sin \omega_N t \quad (3.9)$$

Finally, we have defined the mass ratios of the resonators to the entire sphere

$$\eta_b \equiv \frac{M_b}{\mathcal{M}}, \quad b = 1, \dots, J \quad (3.10)$$

which will be *small parameters* in a real device.

Equations (3.7) are a set of integro-differential equations for the radial deformations of the sphere, $u_a(t)$, and those of the resonators, $z_a(t)$. If we solve them then we obtain at once the complete solution to our general problem by direct substitution of these quantities into (3.5a), then in (3.6a). But before going into the technical details of the solution process let us briefly pause for a qualitative inspection.

Equation (3.7a) shows that the sphere's deformations $u_a(t)$ are made up of two contributions: one due to the action of *external agents* (GWs or other), contained in $u_a^{\text{external}}(t)$, and another one due to coupling to the resonators. The latter is commanded by the small parameters η_b , and correlates to *all* of the sphere's spheroidal eigenmodes through the kernel matrix $K_{ab}(t)$. This has consequences for GW detectors, for even though GWs only couple to quadrupole and monopole³ spheroidal modes of the *free* sphere [5,10,11], attachment of resonators causes, as we see, a well defined amount of energy to be transferred from these into other modes of the antenna, and conversely, these modes back-act on the former. As we shall shortly prove, such effects can be minimised by suitable *tuning* of the resonators' frequencies, but outright neglect of them results in inaccurate conclusions about the system dynamics.

A. Laplace transform domain equations

We now take up the problem of solving equations (3.7). Equation (3.7a) is an integral equation belonging in the general category of Volterra equations [29], but a series solution to it in ascending powers of η_b by iterative substitution of $u_b(t)$ into the kernel integral is not viable due to the *dynamical* contribution of $z_b(t)$, which is in turn governed by the *differential* equation (3.7b). A better suited method to address this *integro-differential* system is to Laplace-transform equations (3.7). We denote the Laplace transform of a generic function of time $f(t)$ with a *caret* ($\hat{}$) on its symbol, e.g.,

³ Monopole modes only exist in scalar-tensor theories of gravity, such as e.g. Brans–Dicke [28]; General Relativity does not belong in this category.

$$\hat{f}(s) \equiv \int_0^\infty f(t) e^{-st} dt \quad (3.11)$$

and make the assumption that the system is at rest before an instant of time, $t = 0$, say, or

$$\mathbf{u}(\mathbf{x}, 0) = \dot{\mathbf{u}}(\mathbf{x}, 0) = z_a(0) = \dot{z}_a(0) = 0 \quad (3.12)$$

Equations (3.7) are then recast in the equivalent form

$$\hat{u}_a(s) = \hat{u}_a^{\text{external}}(s) - \sum_{b=1}^J \eta_b \hat{K}_{ab}(s) [\hat{z}_b(s) - \hat{u}_b(s)] \quad (3.13a)$$

$$s^2 \hat{z}_a(s) = -\Omega_a^2 [\hat{z}_a(s) - \hat{u}_a(s)] + \hat{\xi}_a(s), \quad a = 1, \dots, J \quad (3.13b)$$

for which use has been made of the *convolution theorem* for Laplace transforms⁴. A further simplification is accomplished if we consider that we shall in practice be only concerned with the *measurable* quantities

$$q_a(t) \equiv z_a(t) - u_a(t), \quad a = 1, \dots, J \quad (3.14)$$

representing the resonators' actual elastic deformations —cf. Figure 1. It is readily seen that these verify the following:

$$\sum_{b=1}^J \left[\delta_{ab} + \eta_b \frac{s^2}{s^2 + \Omega_a^2} \hat{K}_{ab}(s) \right] \hat{q}_b(s) = -\frac{s^2}{s^2 + \Omega_a^2} \hat{u}_a^{\text{external}}(s) + \frac{\hat{\xi}_a(s)}{s^2 + \Omega_a^2}, \quad a = 1, \dots, J \quad (3.15)$$

where

$$\hat{u}_a^{\text{external}}(s) = \sum_{\alpha} \left\{ \sum_N \frac{1}{s^2 + \omega_N^2} f_{\text{external},N}^{(\alpha)} [\mathbf{n}_a \cdot \mathbf{u}_N(\mathbf{x}_a)] \right\} \hat{g}_{\text{external}}^{(\alpha)}(s) \quad (3.16)$$

and

$$\hat{K}_{ab}(s) = \sum_N \frac{\Omega_b^2}{s^2 + \omega_N^2} [\mathbf{n}_b \cdot \mathbf{u}_N^*(\mathbf{x}_b)] [\mathbf{n}_a \cdot \mathbf{u}_N(\mathbf{x}_a)] \quad (3.17)$$

which ensue directly from (3.8), (3.9) and the definition (3.11).

Equations (3.15) constitute a significant simplification of the original problem, as they are a set of just J *algebraic* rather than integral or differential equations. We must solve them for the unknowns $\hat{q}_a(s)$, then perform *inverse Laplace transforms* to revert to $q_a(t)$. But we note that Equations (3.15) and (3.16) indicate that the Laplace transform functions we shall be concerned with are of the *rational* class, i.e., they are *quotients of polynomials* in s . This greatly facilitates the latter step (Laplace transform inversion), as it can in this case be obtained by the *calculus of residues* [30].

Determination of the *poles* of $\hat{q}_a(s)$ is thus required in the first place. Clearly, poles correspond to those values of s for which the matrix in square brackets in the lhs of (3.15) is *singular*⁵ or, equivalently, to the zeroes of its determinant:

$$\Delta(s) \equiv \det \left[\delta_{ab} + \eta_b \frac{s^2}{s^2 + \Omega_a^2} \hat{K}_{ab}(s) \right] = 0, \quad \text{Poles} \quad (3.18)$$

As is well known, the *imaginary parts* of the *poles* are the system *characteristic frequencies*, or resonances [31]; *residues* at such poles determine the specific weight of the respectively associated modes in the system response to a given external agent.

The procedure's general guidelines to solve the problem are thus clear-cut. The details of its actual implementation are however not obvious, so we now come to them. We begin with the simplest case, i.e., a perfect sphere with perfectly tuned identical resonators.

⁴ This theorem states, it is recalled, that the Laplace transform of the convolution product of two functions is the arithmetic product of their respective Laplace transforms.

⁵ I.e., non-invertible.

IV. PERFECT SPHERE, IDENTICAL RESONATORS, IDEAL TUNING

We first consider this highly idealised situation as a suitable starting point to address more realistic practical instances, which we naturally do *not* expect to depart excessively from that ideality, anyway. Moreover this simpler analysis will be very interesting *conceptually*, as all the major (coarse grain) characteristics of the system will emerge out of it.

In a perfect sphere the frequencies of the eigenmodes can be classified as l -pole series of ascending harmonics, each frequency in a given series being $(2l+1)$ -fold degenerate. GWs exclusively couple to *spheroidal* eigenmodes [11], and our resonators are assumed to be sensitive to *radial* deformations of the sphere, so only *spheroidal frequencies* will concern us here. Following the notation of reference [10], we denote by ω_{nl} the n -th harmonic of the l -th l -pole series, whose associated $2l+1$ eigenfunctions have the following radial projections:

$$\mathbf{n} \cdot \mathbf{u}_{nlm}(\mathbf{x}) = A_{nl}(r) Y_{lm}(\theta, \varphi) \quad (4.1)$$

where $Y_{lm}(\theta, \varphi)$ are spherical harmonics [26], and $A_{nl}(r)$ are given in [10]. Degeneracy of the eigenfrequencies ω_{nl} enables direct summation over the degeneracy index m in (3.17), so that

$$\hat{K}_{ab}(s) = \sum_{nl} \frac{\Omega_b^2}{s^2 + \omega_{nl}^2} |A_{nl}(R)|^2 \frac{2l+1}{4\pi} P_l(\mathbf{n}_a \cdot \mathbf{n}_b) \equiv \sum_{nl} \frac{\Omega_b^2}{s^2 + \omega_{nl}^2} \chi_{ab}^{(nl)} \quad (4.2)$$

for a *perfectly symmetric sphere*. Here, use has been made of the summation formula (A1) —see Appendix below. Our next assumption is that all the resonators are *identical*, or

$$\eta_1 = \dots = \eta_J \equiv \eta, \quad \Omega_1 = \dots = \Omega_J \equiv \Omega \quad (4.3)$$

The fundamental idea behind using resonators is to have them tuned to one of the frequencies of the sphere's spectrum, so we now make our third hypothesis:

$$\Omega = \omega_{n_0 l_0} \quad (4.4)$$

In a GW detector it will only make sense to choose $l_0 = 0$ or $l_0 = 2$, of course, and have n_0 refer to the first or perhaps second harmonic [12]. We keep the generic expression (4.4) for the time being to encompass all the possibilities within a single formalism, and to make room for calibration signals, too.

Based on the above three hypotheses —i.e., perfect spherical symmetry plus equations (4.3) and (4.4)—, we can now rewrite equation (3.17):

$$\sum_{b=1}^J \left[\delta_{ab} + \eta \sum_{nl} \frac{\Omega^2 s^2}{(s^2 + \Omega^2)(s^2 + \omega_{nl}^2)^2} \chi_{ab}^{(nl)} \right] \hat{q}_b(s) = -\frac{s^2}{s^2 + \Omega^2} \hat{u}_a^{\text{external}}(s) + \frac{\hat{\xi}_a(s)}{s^2 + \Omega_a^2}, \quad (\Omega = \omega_{n_0 l_0}) \quad (4.5)$$

Equation (3.18) for the system resonances can also be recast in a more convenient form:

$$\Delta(s) \equiv \det \left[\delta_{ab} + \eta \frac{\Omega^2 s^2}{(s^2 + \Omega^2)^2} \chi_{ab}^{(n_0 l_0)} + \eta \sum_{nl \neq n_0 l_0} \frac{\Omega^2 s^2}{(s^2 + \Omega^2)(s^2 + \omega_{nl}^2)^2} \chi_{ab}^{(nl)} \right] = 0 \quad (4.6)$$

To find an *analytic* expression for the roots of (4.6) is an impossible task, so we resort to a *perturbative expansion* in the small “coupling constant” η . As we shall now see, much light is shed onto the physics of the problem as we proceed with that expansion.

V. FREQUENCY SPECTRUM

Let us formally state the *essential* fact that the resonators are much less massive than the sphere, which is the basis for *all* the considerations from now on in this paper:

$$\eta \ll 1 \quad (5.1)$$

It is clear from the structure of equation (4.6) that vanishing of $\Delta(s)$ will require s to be such that the denominators in the fractions within square brackets there be proportional to η ; otherwise it will not be possible to have $\Delta(s) = 0$

for *arbitrarily small* values of η , since δ_{ab} is of course a regular matrix. But this points to a sharp distinction between roots which are close to $s = \pm i\Omega = \pm i\omega_{n_0 l_0}$, and roots which are close to $s = \pm i\omega_{nl}$ ($nl \neq n_0 l_0$). The former's *degree of proximity* to $\pm i\Omega$ is of order $\eta^{1/2}$, while the latter's proximity to $\pm i\omega_{nl}$ is of order η , instead. We thus correspondingly distinguish the following two categories of roots:

$$s_0^2 = -\Omega^2 \left(1 + \chi_{\frac{1}{2}} \eta^{1/2} + \chi_1 \eta + \dots \right) \quad (\Omega = \omega_{n_0 l_0}) \quad (5.2a)$$

$$s_{nl}^2 = -\omega_{nl}^2 \left(1 + b_1^{(nl)} \eta + b_2^{(nl)} \eta^2 + \dots \right) \quad (nl \neq n_0 l_0) \quad (5.2b)$$

The coefficients $\chi_{\frac{1}{2}}, \chi_1, \dots$ and $b_1^{(nl)}, b_2^{(nl)}, \dots$ can be calculated recursively, starting from the first. As we now show, these two categories of roots present qualitatively different characteristics. We consider them separately.

A. Roots near Ω

Upon substitution of (5.2a) into (4.6) it is readily seen that $\chi_{\frac{1}{2}}$ is a solution to the algebraic equation

$$\det \left[\delta_{ab} - \frac{1}{\chi_{\frac{1}{2}}^2} \chi_{ab}^{(n_0 l_0)} \right] = 0 \quad (5.3)$$

So $\chi_{\frac{1}{2}}^2$ are the *eigenvalues* of the matrix $\chi_{ab}^{(n_0 l_0)}$, which happens to be non-negative definite —see Appendix. There are of course J of these, some of which may be repeated (*degenerate*), or null. This means that we get J *pairs of roots* of the type s_0 in (5.2a) lying on the imaginary axis of the complex s -plane *symmetrically* (to order $\eta^{1/2}$) around $\pm i\Omega$ —see Figure 2. The system resonant frequencies can thus be represented by the pairs

$$\omega_{a\pm}^2 = \Omega^2 \left(1 \pm \sqrt{\frac{2l+1}{4\pi}} |A_{n_0 l_0}(R)| \zeta_a \eta^{1/2} \right) + O(\eta), \quad a = 1, \dots, J \quad (5.4)$$

where ζ_a^2 are the *eigenvalues* of the matrix $P_{l_0}(\mathbf{n}_a \cdot \mathbf{n}_b)$, and $O(\eta)$ stands for the higher order terms in (5.2a).

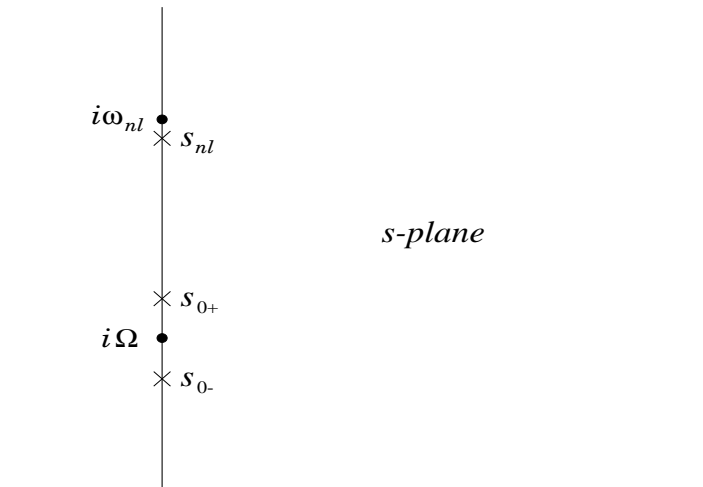


FIG. 2. Qualitative situation of the roots in the complex s -plane. Dots correspond to the *free* sphere's frequencies, while crosses correspond to *coupled* system frequencies. Roots near the tuning frequency Ω come in pairs (we draw just one, corresponding to one single resonator, to avoid unnecessary complication at this stage), while roots near other (higher) free sphere frequencies are *downshifted* rather than split, though the effect is altogether weaker in this case —see equation (5.2b).

Equation (5.4) very much reminds us of a familiar result in cylindrical bar theory [17]: attachment of a resonator to the bar's end face causes the latter's characteristic resonance frequency to split up into a symmetric pair around the original value, the amount of relative shift being proportional to $\eta^{1/2}$. As we now see, in a spherical body the number of frequency pairs equals the number of resonators, it is of the same order of magnitude ($\eta^{1/2}$), and is precisely controlled by the geometry dependent eigenvalues ζ_a .

It must however be cautioned that (5.4) *is not an exact* result, but the *dominant approximation* in an ascending series in powers of $\eta^{1/2}$. If better accuracy is needed then higher terms in (5.2a) must be calculated. For example, the *next order* correction to s_0^2 in (5.2a) is

$$\chi_{1,a} = \frac{1}{2} \left[\chi_{\frac{1}{2},a}^2 - \sum_{nl \neq n_0 l_0} \frac{\Omega^2}{\omega_{nl}^2 - \Omega^2} \tilde{\chi}_{aa}^{(nl)} \right], \quad a = 1, \dots, J \quad (5.5)$$

corresponding to the a -th root of the previous order, equation (5.3). In this formula we have $\tilde{\chi}_{aa}^{(nl)}$, which stands for the a -th diagonal element of the matrix $\chi_{ab}^{(nl)}$ in the (abstract) system of axes in which $\chi_{ab}^{(n_0 l_0)}$ is diagonal.

The second order corrections (5.5) are seen to be equal for the two members of the frequency pairs (5.4), as they only depend on $\chi_{\frac{1}{2}}^2$. They thus result in *rigid shifts* for both of them. More substantial, the actual value of these corrections involves the *whole spectrum* of spheroidal eigenfrequencies and wavefunctions. This should not be considered surprising on general grounds⁶, but to find this result has required us to model the system dynamics in a more elaborate conceptual structure than has been considered so far in the literature [20,33,34]. The physical interpretation of (5.5) is that the attachment of resonators causes a certain level of *intercommunication* between different vibration eigenmodes of the sphere, even if the resonators are accurately tuned to one of the spectral frequencies. This “cross talk” between modes has consequences for non-tuned modes, as we shall see in the next subsection, as well as for tuned modes, as we see in (5.5). The practical relevance of these higher order corrections will naturally be dictated by the precision of measurements in a real GW antenna. As of this date, the experimental data available on such devices as described here is to our knowledge limited to the *TIGA* prototype data [21], but the experimental conditions reported [22] are not sufficiently fine tuned to guarantee that corrections of order η to fit the data are really meaningful—see section 8 below. This is surely the reason why errors in the formulas given by other authors for system frequencies [35] have passed unnoticed so far.

B. Roots near $\omega_{nl} \neq \Omega$

We now come to the other roots, equation (5.2b). If the latter is substituted into (4.6) then we readily see that $b_1^{(nl)}$ satisfies the algebraic equation

$$\det \left[\frac{\Omega^2 - \omega_{nl}^2}{\omega_{nl}^2} b_1^{(nl)} \delta_{ab} - \chi_{ab}^{(nl)} \right] = 0 \quad (5.6)$$

which is again an eigenvalue equation, having J solutions. Since the eigenvalues of the matrix $\chi_{ab}^{(nl)}$ are either positive or null (see Appendix) it follows that $b_1^{(nl)}$ either has the same sign as $(\Omega^2 - \omega_{nl}^2)$ or is zero, respectively. Thus for example, if Ω is chosen equal to the lowest frequency of the spectrum (first quadrupole harmonic, ω_{12}) then the system frequencies close to ω_{nl} will be slightly *downshifted* relative to their original value ω_{nl} . This is schematically represented in Figure 2.

We see again in equation (5.6) that the presence of resonators does indeed affect the whole spectrum of the free sphere, though with an intensity of coupling which differs between tuned and non-tuned modes by factors of order $\eta^{1/2}$. We shall not go into any more depth in the analysis of these fine structure details in this paper.

VI. SYSTEM RESPONSE TO A GRAVITATIONAL WAVE

Our next concern is the actual system response when it is acted upon by an incoming GW, i.e., which are the *amplitudes* of the excited modes, whose frequencies we have just estimated, and how do they relate to the GW amplitudes $g^{(lm)}(t)$. To this end we must find the inverse Laplace transform of $\hat{q}_a(s)$:

$$\hat{q}_a(s) = - \sum_{b=1}^J \left[\delta_{ab} + \eta \sum_{nl} \frac{\Omega^2 s^2}{(s^2 + \Omega^2)(s^2 + \omega_{nl}^2)} \chi_{ab}^{(nl)} \right]^{-1} \left(\frac{s^2}{s^2 + \Omega^2} \hat{u}_b^{\text{GW}}(s) - \frac{\hat{\xi}_a(s)}{s^2 + \Omega_a^2} \right), \quad a = 1, \dots, J \quad (6.1)$$

⁶ Second order perturbative corrections to eigenvalues often show this feature—recall e.g. energy level corrections in Quantum Mechanics [32].

as follows from (4.5), where $\hat{u}_b^{\text{external}}(s)$ has been substituted by $\hat{u}_b^{\text{GW}}(s)$, which is in its turn given by

$$\hat{u}_b^{\text{GW}}(s) = \sum_{\substack{l=0 \text{ and } 2 \\ m=-l, \dots, l}} \left(\sum_{n=1}^{\infty} \frac{a_{nl} A_{nl}(R)}{s^2 + \omega_{nl}^2} \right) Y_{lm}(\mathbf{n}_b) \hat{g}^{(lm)}(s), \quad b = 1, \dots, J \quad (6.2)$$

according to (3.4b), (3.5b) and (4.1). Clearly, from (2.9) we also have

$$\hat{\xi}_a^{\text{GW}}(s) = R \sum_{\substack{l=0 \text{ and } 2 \\ m=-l, \dots, l}} Y_{lm}(\mathbf{n}_a) \hat{g}^{(lm)}(s), \quad a = 1, \dots, J \quad (6.3)$$

In order to ease the notation we can combine (6.1) and (6.2) into a more compact form:

$$\hat{q}_a(s) = \sum_{\substack{l=0 \text{ and } 2 \\ m=-l, \dots, l}} \hat{\Phi}_a^{(lm)}(s) \hat{g}^{(lm)}(s), \quad a = 1, \dots, J \quad (6.4)$$

with, obviously,

$$\hat{\Phi}_a^{(lm)}(s) \equiv - \sum_{b=1}^J \left[\delta_{ab} + \eta \sum_{nl} \frac{\Omega^2 s^2}{(s^2 + \Omega^2)(s^2 + \omega_{nl}^2)} \chi_{ab}^{(nl)} \right]^{-1} \frac{s^2}{s^2 + \Omega^2} \left(-\frac{R}{s^2} + \sum_{n=1}^{\infty} \frac{a_{nl} A_{nl}(R)}{s^2 + \omega_{nl}^2} \right) Y_{lm}(\mathbf{n}_b) \quad (6.5)$$

We thus have, by the convolution theorem again,

$$q_a(t) = \sum_{lm} \int_0^t \hat{\Phi}_a^{(lm)}(t-t') g^{(lm)}(t') dt', \quad a = 1, \dots, J \quad (6.6)$$

where $\hat{\Phi}_a^{(lm)}(t)$ is the *inverse Laplace transform* of (6.5). Despite its complexity, $\hat{\Phi}_a^{(lm)}(s)$ is a *rational function* of s , and therefore its inverse Laplace transform can be calculated, as already advanced in section 3, by the *residue theorem* through the formula [31]

$$\Phi_a^{(lm)}(t) = 2\pi i \sum \left\{ \text{residues of } \left[\hat{\Phi}_a^{(lm)}(s) e^{st} \right] \text{ at its poles in complex } s\text{-plane} \right\} \quad (6.7)$$

The *poles* in this formula happen to be *exclusively* those of equations (5.2), and there are *no* poles either at $s^2 = -\Omega^2$ or at $s^2 = -\omega_{nl}^2$, for divergences compensate each other in numerators and denominators in (6.5) at those points. Our next step is thus to calculate the corresponding *residues*. This is a relatively simple, but considerably laborious task, the details of which will be omitted here. We just quote the results and directly move on to their discussion.

One can see that $\Phi_a^{(lm)}(t)$ has the following general structure:

$$\Phi_a^{(lm)}(t) \propto \eta^{-1/2} \sum_{\zeta_c \neq 0} (\sin \omega_{c+} t - \sin \omega_{c-} t) \delta_{ll_0} + O(0) \quad (6.8)$$

where $\omega_{c\pm}$ are given in (5.4), and the sum above *excludes* terms associated to null eigenvalues ζ_c . The term $O(0)$ stands for higher order corrections, which in this case happen to be of order zero in η . But let us look at the important *qualitative* consequences of (6.8).

- i) The resonators' motions occur with a mechanical amplification factor of $\eta^{-1/2}$ relative to the driving GW amplitudes $g^{(lm)}(t)$, provided the resonator frequency Ω is tuned to a monopole or quadrupole sphere frequency — see the factor δ_{ll_0} in (6.8). If other frequencies are chosen for tuning then there is no coupling to GWs to this order, but weaker by factors of $\eta^{1/2}$, at least.
- ii) The spectral composition of these motions is dominated by the symmetric frequency pairs $\omega_{c\pm}$ into which the tuned frequency $\omega_{n_0 l_0} = \Omega$ splits up as a consequence of the resonators' presence. The maximum number of such frequency pairs is $(2l_0+1)$, *even if the number of resonators, J , is larger than this figure*. This is because $(2l_0+1)$ is the *maximum* number of non-null eigenvalues ζ_c — cf. Appendix.

iii) Higher order terms, symbolised by $O(0)$ in (6.8), encompass couplings to all the non-tuned modes, whose frequencies are given by (5.2b), as well as corrections of the same order of magnitude in the tuned mode. The latter include in particular modes corresponding to a null eigenvalue ζ_c , which are guaranteed to be present whenever $J > 2l_0 + 1$. As we shall shortly see, an example of this is provided by the *TIGA* layout [21].

Higher order corrections are considerably more difficult to address than first order, and we shall not attempt a closer approach to them in this paper. So let us continue with the investigation of the system response to lowest order. Given the above discussion, it is expedient to recast (6.4) in the form

$$\hat{q}_a(s) = \eta^{-1/2} \sum_{l,m} \hat{\Lambda}_a^{(lm)}(s; \Omega) \hat{g}^{(lm)}(s) + O(0), \quad a = 1, \dots, J \quad (6.9)$$

where Ω will be tuned to either a monopole ($\Omega = \omega_{n0}$) or a quadrupole ($\Omega = \omega_{n2}$) frequency of the free sphere's spheroidal spectrum. We consider the two possibilities successively.

A. Monopole gravitational radiation sensing

General Relativity, as is well known, forbids monopole GW radiation. More general *metric* theories, e.g. Brans-Dicke [28], do however predict this kind of radiation. It appears that a spherical antenna is potentially sensitive to monopole waves, so it can serve the purpose of thresholding, or eventually detecting them. This clearly requires that the resonator set be tuned to a monopole harmonic of the sphere, i.e.,

$$\Omega = \omega_{n0}, \quad (l_0 = 0) \quad (6.10)$$

where n tags the chosen harmonic —most likely the first ($n = 1$) in a thinkable device.

Since $P_0(z) \equiv 1$ (for all z) the eigenvalues of $P_0(\mathbf{n}_a \cdot \mathbf{n}_b)$ are, clearly,

$$\zeta_1^2 = J, \quad \zeta_2^2 = \dots = \zeta_J^2 = 0 \quad (6.11)$$

for *any resonator distribution*. The tuned mode frequency thus splits into a *single* strongly coupled pair:

$$\omega_{\pm}^2 = \omega_{n0}^2 \left(1 \pm \sqrt{\frac{J}{4\pi}} |A_{n0}(R)| \eta^{1/2} \right) + O(\eta), \quad \Omega = \omega_{n0} \quad (6.12)$$

The Λ -matrix of equation (6.9) is easily seen to be in this case

$$\hat{\Lambda}_a^{(lm)}(s; \omega_{n0}) = (-1)^J \frac{a_{n0}}{\sqrt{J}} \frac{1}{2} \left[(s^2 + \omega_+^2)^{-1} - (s^2 + \omega_-^2)^{-1} \right] \delta_{l0} \delta_{m0} \quad (6.13)$$

whence the system response is

$$\hat{q}_a(s) = \eta^{-1/2} \frac{(-1)^J}{\sqrt{J}} a_{n0} \frac{1}{2} \left[(s^2 + \omega_+^2)^{-1} - (s^2 + \omega_-^2)^{-1} \right] \hat{g}^{(00)}(s) + O(0), \quad a = 1, \dots, J \quad (6.14)$$

regardless of resonator positions. The *overlap coefficient* a_{n0} is calculated by means of formulas given in [10], and has dimensions of length. By way of example, $a_{10}/R \simeq 0.214$, and $a_{20}/R \simeq -0.038$ for the first two harmonics.

A few interesting facts are displayed by equation (6.14). First, as we have already stressed, it is seen that if the resonators are tuned to a monopole *detector* frequency then only monopole *wave amplitudes* couple strongly to the system, even if quadrupole radiation amplitudes are significantly high at the observation frequencies ω_{\pm} . Also, the amplitudes $\hat{q}_a(s)$ are equal for all a , as corresponds to the spherical symmetry of monopole sphere's oscillations, and are proportional to $J^{-1/2}$, a factor we should indeed expect as an indication that GW *energy* is evenly distributed amongst all the resonators. A *single* transducer suffices to experimentally determine the only monopole GW amplitude $\hat{g}^{(00)}(s)$, of course, but (6.14) provides the system response if more than one sensor is mounted on the antenna for whatever reasons.

B. Quadrupole gravitational radiation sensing

We now consider the more interesting case of quadrupole motion sensing. We thus take

$$\Omega = \omega_{n2} , \quad (l_0 = 2) \quad (6.15)$$

where n labels the chosen harmonic —most likely the first ($n=1$) or the second ($n=2$) in a practical system. The evaluation of the Λ -matrix is now considerably more involved, yet a remarkably elegant form is found for it:

$$\hat{\Lambda}_a^{(lm)}(s; \omega_{n2}) = (-1)^N \sqrt{\frac{4\pi}{5}} a_{n2} \sum_{b=1}^J \left\{ \sum_{\zeta_c \neq 0} \frac{1}{2} \left[(s^2 + \omega_{c+}^2)^{-1} - (s^2 + \omega_{c-}^2)^{-1} \right] \frac{v_a^{(c)} v_b^{(c)*}}{\zeta_c} \right\} Y_{2m}(\mathbf{n}_b) \delta_{l2} \quad (6.16)$$

where $v_a^{(c)}$ is the c -th normalised eigenvector of $P_2(\mathbf{n}_a \cdot \mathbf{n}_b)$, associated to the *non-null* eigenvalue ζ_c^2 . Let us stress once more that equation (6.16) explicitly shows that at most 5 pairs of modes, of frequencies $\omega_{c\pm}$, couple strongly to quadrupole GW amplitudes, *no matter how many resonators in excess of 5 are mounted on the sphere*. The tidal overlap coefficients a_{2n} can also be calculated, and give for the first two harmonics [23]

$$\frac{a_{12}}{R} = 0.328 , \quad \frac{a_{22}}{R} = 0.106 \quad (6.17)$$

The system response is thus

$$\hat{q}_a(s) = \eta^{-1/2} (-1)^J \sqrt{\frac{4\pi}{5}} a_{n2} \sum_{b=1}^J \left\{ \sum_{\zeta_c \neq 0} \frac{1}{2} \left[(s^2 + \omega_{c+}^2)^{-1} - (s^2 + \omega_{c-}^2)^{-1} \right] \frac{v_a^{(c)} v_b^{(c)*}}{\zeta_c} \right\} \times \\ \times \sum_{m=-2}^2 Y_{2m}(\mathbf{n}_b) \hat{g}^{(2m)}(s) + O(0) , \quad a = 1 \dots, J \quad (6.18)$$

Equation (6.18) is *completely general*, i.e., it is valid for any resonator configuration over the sphere's surface, and for any number of resonators. It describes precisely how all 5 GW amplitudes $\hat{g}^{(2m)}(s)$ interact with all 5 strongly coupled system modes; like before, *only* quadrupole *wave* amplitudes are seen in the detector (to leading order) when $\Omega = \omega_{n2}$, even if the incoming wave carries significant monopole energy at the frequencies $\omega_{c\pm}$.

The consequences of (6.18) are best seen in practical examples, so we now come to a more detailed consideration of two specific resonator distributions.

C. The TIGA configuration

A highly symmetric resonator layout has been proposed and experimentally studied by Merkowitz and Johnson at LSU [19–21], which consists in a set of *six* transducers attached to the six non-parallel pentagonal faces of a *truncated icosahedron*, as shown schematically in Figure 3.

It can be immediately verified that the five non-null eigenvalues of $P_2(\mathbf{n}_a \cdot \mathbf{n}_b)$ are *all equal* for this distribution, and there is a null sixth, too:

$$\zeta_{-2}^2 = \dots = \zeta_2^2 = \frac{6}{5} , \quad \zeta_6^2 = 0 \quad (TIGA) \quad (6.19)$$

This means that all five pairs of strongly coupled frequencies collapse into a single, five-fold degenerate pair:

$$\omega_{\pm}^2 = \omega_{n2}^2 \left(1 \pm \sqrt{\frac{3}{2\pi}} |A_{n2}(R)| \eta^{1/2} \right) + O(\eta) , \quad a = 1, \dots, 6 \quad (6.20)$$

Degeneracy in this layout is a consequence of its symmetry relative to the quadrupole structure of the GW driving force and the tuned detector modes. It is also not difficult to see that the *TIGA* is the *minimal* configuration with so much degeneracy, as there are no 5 resonator configurations with equivalent symmetry. There are however other non-minimal sets with the same degree of degeneracy —for example 10 resonators on the ten non-parallel faces of a regular icosahedron, etc., see e.g. [33] for further analysis of this and other possibilities.

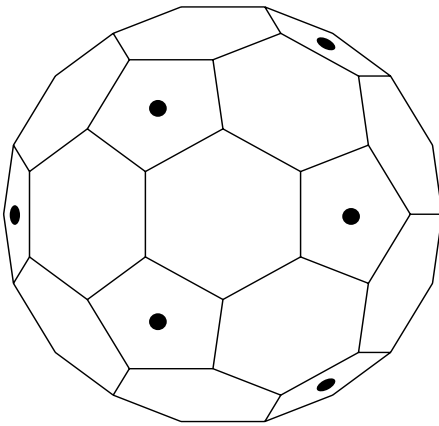


FIG. 3. Schematic view of the *TIGA*: a truncated icosahedron shape with black dots at the resonators' positions.

The normalised eigenvectors associated to the five non-vanishing eigenvalues (6.19), which are the only relevant ones now, are seen to be

$$v_a^{(m)} = \sqrt{\frac{2\pi}{3}} Y_{2m}(\mathbf{n}_a), \quad m = -2, \dots, 2, \quad a = 1, \dots, 6 \quad (\text{TIGA}) \quad (6.21)$$

The system response is thus given by

$$\hat{q}_a(s) = \eta^{-1/2} \sqrt{\frac{2\pi}{3}} a_{n2} \frac{1}{2} \left[(s^2 + \omega_+^2)^{-1} - (s^2 + \omega_-^2)^{-1} \right] \sum_{m=-2}^2 Y_{2m}(\mathbf{n}_a) \hat{g}^{(2m)}(s) + O(0), \quad a = 1 \dots, 6 \quad (6.22)$$

This highly symmetric and remarkably simple formula was obtained for the first time by Merkowitz and Johnson [19,20]. Its scope and range of validity, as well as its uniqueness, are now more firmly established in the light of the present, more elaborate analysis.

Based on equations (6.22) Merkowitz and Johnson define what they call *mode channels*: these are linear combinations of the resonators' readouts which directly yield the GW amplitudes $\hat{g}^{(2m)}(s)$ at the frequencies ω_{\pm} , and they are easily obtained thanks to the orthonormality property of the eigenvectors (6.21). They are

$$\hat{y}^{(m)}(s) \equiv \sum_{a=1}^6 v_a^{(m)*} \hat{q}_a(s) = \eta^{-1/2} a_{n2} \frac{1}{2} \left[(s^2 + \omega_+^2)^{-1} - (s^2 + \omega_-^2)^{-1} \right] \hat{g}^{(2m)}(s) + O(0), \quad m = -2, \dots, 2 \quad (6.23)$$

There naturally are 5 rather than 6 mode channels —as there are 5 quadrupole GW amplitudes—, and it is easy to implement an algorithm to calculate them *on line* from raw detector data. So signal and direction deconvolution methods [5,10,33] can be directly applied to the mode channel set very advantageously. This should be considered one more attractive property of the *TIGA* layout since, as we see in equation (6.18), arbitrary resonator configurations do not generally permit the construction of such mode channels so efficiently.

D. The *PHC* configuration

As we have just seen the TI layout is highly symmetric, and is the minimal set with maximum degeneracy. To accomplish this, however, 6 rather than 5 resonators are required on the sphere's surface. Since there are just 5 quadrupole GW amplitudes one may wonder whether there are alternative layouts with *only* 5 resonators. Equation (6.18) is completely general, so it can be searched for an answer to this question. In reference [23] we made a specific proposal, which we now describe in more detail.

In pursuing a search for 5 resonator sets we found that distributions having a sphere diameter as an axes of *pentagonal symmetry*⁷ exhibit a rather appealing structure. More specifically, let the resonators be located at the spherical positions

⁷ By this we mean resonators are placed along a *parallel* of the sphere every 72°.

$$\theta_a = \alpha \quad (\text{all } a), \quad \varphi_a = (a-1) \frac{2\pi}{5}, \quad a = 1, \dots, 5 \quad (6.24)$$

The eigenvalues and eigenvectors of $P_2(\mathbf{n}_a \cdot \mathbf{n}_b)$ are then

$$\zeta_0^2 = \frac{5}{4} (3 \cos^2 \alpha - 1)^2, \quad \zeta_1^2 = \zeta_{-1}^2 = \frac{15}{2} \sin^2 \alpha \cos^2 \alpha, \quad \zeta_2^2 = \zeta_{-2}^2 = \frac{15}{8} \sin^4 \alpha \quad (6.25a)$$

$$v_a^{(m)} = \sqrt{\frac{4\pi}{5}} \zeta_m^{-1} Y_{2m}(\mathbf{n}_a), \quad m = -2, \dots, 2, \quad a = 1, \dots, 5 \quad (6.25b)$$

so the Λ -matrix is also considerably simple in structure in this case:

$$\hat{\Lambda}_a^{(lm)}(s; \omega_{n2}) = -\sqrt{\frac{4\pi}{5}} a_{n2} \zeta_m^{-1} \frac{1}{2} \left[(s^2 + \omega_{m+}^2)^{-1} - (s^2 + \omega_{m-}^2)^{-1} \right] Y_{2m}(\mathbf{n}_a) \delta_{l2} \quad (PHC) \quad (6.26)$$

where we have used the obvious notation

$$\omega_{m\pm}^2 = \omega_{n2}^2 \left(1 \pm \sqrt{\frac{5}{4\pi}} |A_{n2}(R)| \zeta_m \eta^{1/2} \right) + O(\eta), \quad m = -2, \dots, 2 \quad (6.27)$$

As we see from these formulas, the *five* expected pairs of frequencies actually reduce to *three*, so pentagonal distributions keep a certain degree of degeneracy, too. The most important distinguishing characteristic of the general *pentagonal* layout is best displayed by the explicit system response:

$$\begin{aligned} \hat{q}_a(s) = & -\eta^{-1/2} \sqrt{\frac{4\pi}{5}} a_{n2} \left\{ \frac{1}{2\zeta_0} \left[(s^2 + \omega_{0+}^2)^{-1} - (s^2 + \omega_{0-}^2)^{-1} \right] Y_{20}(\mathbf{n}_a) \hat{g}^{(20)}(s) \right. \\ & + \frac{1}{2\zeta_1} \left[(s^2 + \omega_{1+}^2)^{-1} - (s^2 + \omega_{1-}^2)^{-1} \right] \left[Y_{21}(\mathbf{n}_a) \hat{g}^{(11)}(s) + Y_{2-1}(\mathbf{n}_a) \hat{g}^{(1-1)}(s) \right] \\ & \left. + \frac{1}{2\zeta_2} \left[(s^2 + \omega_{2+}^2)^{-1} - (s^2 + \omega_{2-}^2)^{-1} \right] \left[Y_{22}(\mathbf{n}_a) \hat{g}^{(22)}(s) + Y_{2-2}(\mathbf{n}_a) \hat{g}^{(2-2)}(s) \right] \right\} \quad (6.28) \end{aligned}$$

This equation indicates that *different wave amplitudes selectively couple to different detector frequencies*. This should be considered a very remarkable fact, for it thence follows that simple inspection of the system readout *spectrum*⁸ immediately reveals whether a given wave amplitude $\hat{g}^{2m}(s)$ is present in the incoming signal or not.

Pentagonal configurations also admit *mode channels*, which are easily constructed from (6.28) thanks to the orthonormality property of the eigenvectors (6.25b):

$$\hat{y}^{(m)}(s) \equiv \sum_{a=1}^5 v_a^{(m)*} \hat{q}_a(s) = \eta^{-1/2} a_{n2} \frac{1}{2} \left[(s^2 + \omega_{m+}^2)^{-1} - (s^2 + \omega_{m-}^2)^{-1} \right] \hat{g}^{(2m)}(s) + O(0) \quad (6.29)$$

These are almost identical to the *TIGA* mode channels (6.23), the only difference being that each mode channel comes now at a *single specific* frequency pair $\omega_{m\pm}$. It thus appears that a pentagonal transducer configuration enables signal observations over a somewhat richer frequency band than does the *TIGA*.

Based on these facts one may next ask which is a suitable transducer distribution with an axis of pentagonal symmetry. In Figure 4 we give a plot of the eigenvalues (6.25a) as a function of α , the angular distance of the resonator set from the symmetry axis. Several criteria may be adopted to select a specific choice in view of this graph. An interesting one was proposed by us in reference [23] with the following argument. If for ease of mounting, stability, etc., it is desirable to have the detector milled into a close-to-spherical *polyhedral* shape⁹ then polyhedra with axes of pentagonal symmetry must be searched. The number of quasi regular *convex* polyhedra is of course finite—there actually are only 18 of them [36,37]—, and we found a particularly appealing one in the so called *pentagonal hexacontahedron* (*PHC*), which we see in Figure 5, left. This is a 60 face polyhedron, whose faces are the identical *irregular pentagons* on the right of the Figure. The *PHC* admits an *inscribed sphere* which is tangent to each face

⁸ In a noiseless system, of course

⁹ This is the philosophy suggested and experimentally implemented by Merkwitz and Johnson at *LSU*.

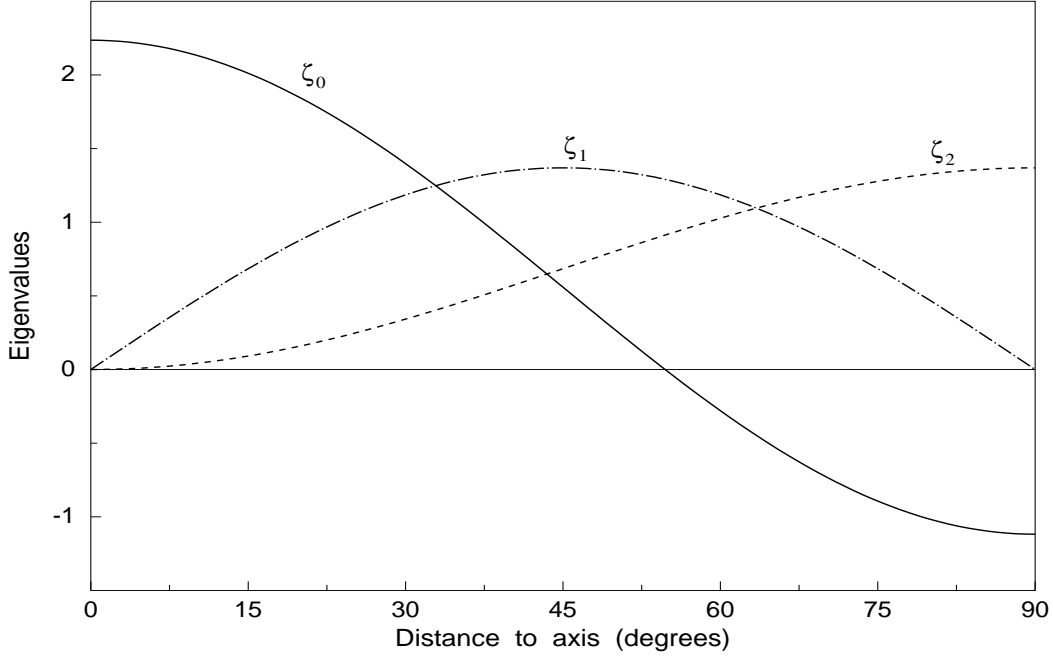


FIG. 4. The three distinct eigenvalues ζ_m ($m=0,1,2$) as functions of the distance of the resonator parallel’s co-latitude α relative to the axis of symmetry of the distribution, cf. equation (6.25a).

at the central point marked in the Figure. It is, clearly, to this point that a resonator should be attached so as to simulate an as perfect as possible spherical distribution.

The *PHC* is considerably spherical: the ratio of its volume to that of the inscribed sphere is 1.057, which quite favourably compares to the value of 1.153 for the ratio of the *circumscribed* sphere to the TI volume. If we now request that the frequency pairs $\omega_{m\pm}$ be as *evenly spaced* as possible, compatible with the *PHC* face orientations, then we must choose $\alpha = 67.617^\circ$, whence

$$\omega_{0\pm} = \omega_{12} \left(1 \pm 0.5756 \eta^{1/2} \right), \quad \omega_{1\pm} = \omega_{12} \left(1 \pm 0.8787 \eta^{1/2} \right), \quad \omega_{2\pm} = \omega_{12} \left(1 \pm 1.0668 \eta^{1/2} \right) \quad (6.30)$$

for instance for $\Omega = \omega_{12}$, the first quadrupole harmonic. In Figure 6 we display this frequency spectrum together with the multiply degenerate *TIGA* for comparison. The frequency span of both distributions is naturally comparable, yet the *PHC* is slightly broader.

The criterion leading to the *PHC* proposal is of course not unique, and alternatives can be considered. For example, if the 5 faces of a regular icosahedron are selected for sensor mounting ($\alpha = 63.45^\circ$) then a four-fold degenerate pair plus a single non-degenerate pair is obtained; if the resonator parallel is 50° or 22.6° away from the “north pole” then the three frequencies ω_{0+} , ω_{1+} , and ω_{2+} are equally spaced; etc. The number of choices is virtually infinite if the sphere is not milled into a polyhedral shape.

Let us finally recall that the complete *PHC* proposal [23] was made with the idea of building an as complete as possible spherical GW antenna, which amounts to making it sensitive at the first *two* quadrupole frequencies *and* at the first monopole one. This would take advantage of the good sphere cross section at the second quadrupole harmonic [12], and would enable measuring (or thresholding) eventual monopole GW radiation. Now, the system *pattern matrix* $\hat{\Lambda}_a^{(lm)}(s; \Omega)$ has *identical structure* for all the harmonics of a given l series —see (6.13) and (6.16)—, and so too identical criteria for resonator layout design apply to either set of transducers, respectively tuned to ω_{12} and ω_{22} . The *PHC* proposal is best described graphically in Figure 5: a *second* set of resonators, tuned to the second quadrupole harmonic ω_{22} can be placed in an equivalent position in the “southern hemisphere”, and an eleventh resonator tuned to the first monopole frequency ω_{10} is added at an arbitrary position. It is not difficult to see, by the general methods outlined earlier on in this paper, that cross interaction between these three sets of resonators is only *second order* in $\eta^{1/2}$, therefore weak.

A spherical GW detector with such a set of altogether 11 transducers would be a very complete multi-mode multi-frequency device with an unprecedented capacity as an individual antenna. Amongst other it would practically enable monitoring of coalescing binary *chirp* signals by means of a rather robust double passage method [38], a prospect

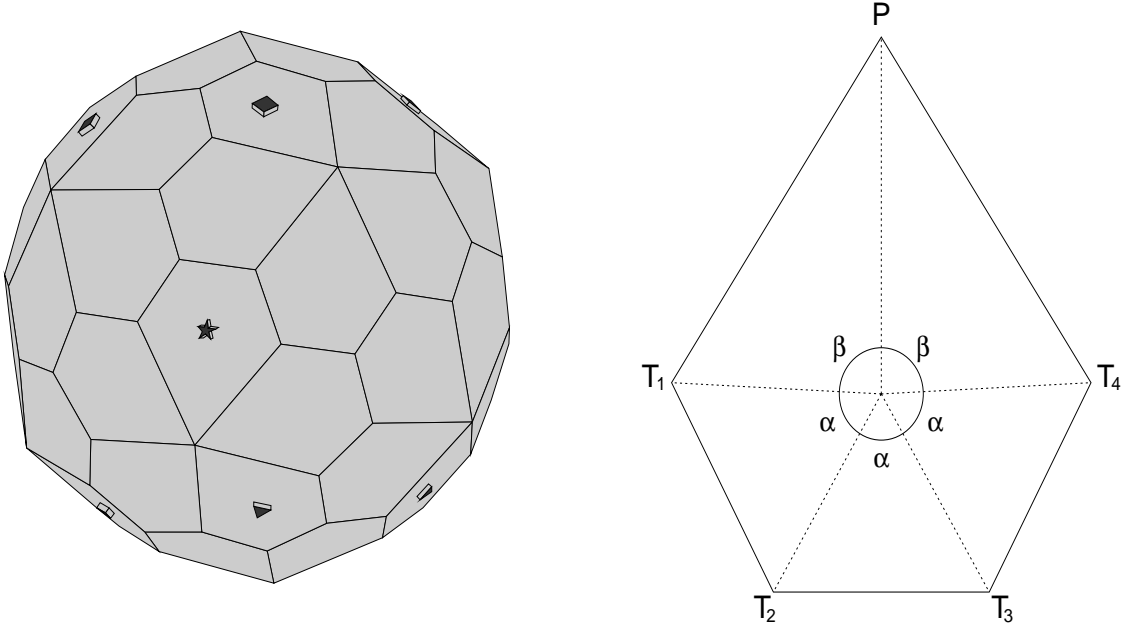


FIG. 5. To the left, the *pentagonal hexacontahedron* shape. Certain faces are marked to indicate resonator positions in a specific proposal —see text— as follows: a *square* for resonators tuned to the first quadrupole frequency, a *triangle* for the second, and a *star* for the monopole. On the right we see the (pentagonal) face of the polyhedron. A few details about it: the confluence point of the dotted lines at the centre is the tangency point of the *inscribed* sphere to the *PHC*; the labeled angles have values $\alpha = 61.863^\circ$, $\beta = 87.205^\circ$; the angles at the *T*-vertices are all equal, and their value is 118.1366° , while the angle at *P* is 67.4536° ; the ratio of a long edge (e.g. PT_1) to a short one (e.g. T_1T_2) is 1.74985, and the radius of the inscribed sphere is *twice* the long edge of the pentagon, $R = 2PT_1$.

which was considered so far possible only with broadband long baseline laser interferometers [39,40], and is almost unthinkable with currently operating cylindrical bars.

VII. A CALIBRATION SIGNAL: HAMMER STROKE

This section is a brief digression from the main streamline of the paper. We propose to assess now the system response to a particular, but useful, calibration signal: a perpendicular *hammer stroke*. After a few general considerations we describe the situation in a *TIGA* and in a *PHC* configuration.

We first go back to equation (3.15) and replace $\hat{u}_a^{\text{external}}(s)$ in its rhs with that corresponding to a hammer stroke, which is easily calculated thanks to (3.4c), (3.5c), and (3.16); the result is

$$\hat{u}_a^{\text{stroke}}(s) = - \sum_{nl} \frac{f_0}{s^2 + \omega_{nl}^2} |A_{nl}(R)|^2 P_l(\mathbf{n}_a \cdot \mathbf{n}_0), \quad a = 1, \dots, J \quad (7.1)$$

where \mathbf{n}_0 are the spherical coordinates of the hit point on the sphere, and $f_0 \equiv \mathbf{n}_0 \cdot \mathbf{f}_0 / \mathcal{M}$. Clearly, the hammer stroke excites *all* of the sphere's vibration eigenmodes, as it has a completely flat spectrum.

The coupled system resonances are of course those already calculated in section 6, and the same procedures described there for a GW excitation can be pursued now to obtain

$$\hat{q}_a(s) = \eta^{-1/2} (-1)^{J-1} \sqrt{\frac{2l+1}{4\pi}} f_0 |A_{nl}(R)| \times \\ \times \sum_{b=1}^J \left\{ \sum_{\zeta_c \neq 0} \frac{1}{2} \left[(s^2 + \omega_{c+}^2)^{-1} - (s^2 + \omega_{c-}^2)^{-1} \right] \frac{v_a^{(c)} v_b^{(c)*}}{\zeta_c} \right\} P_l(\mathbf{n}_b \cdot \mathbf{n}_0) + O(0), \quad a = 1 \dots, J \quad (7.2)$$

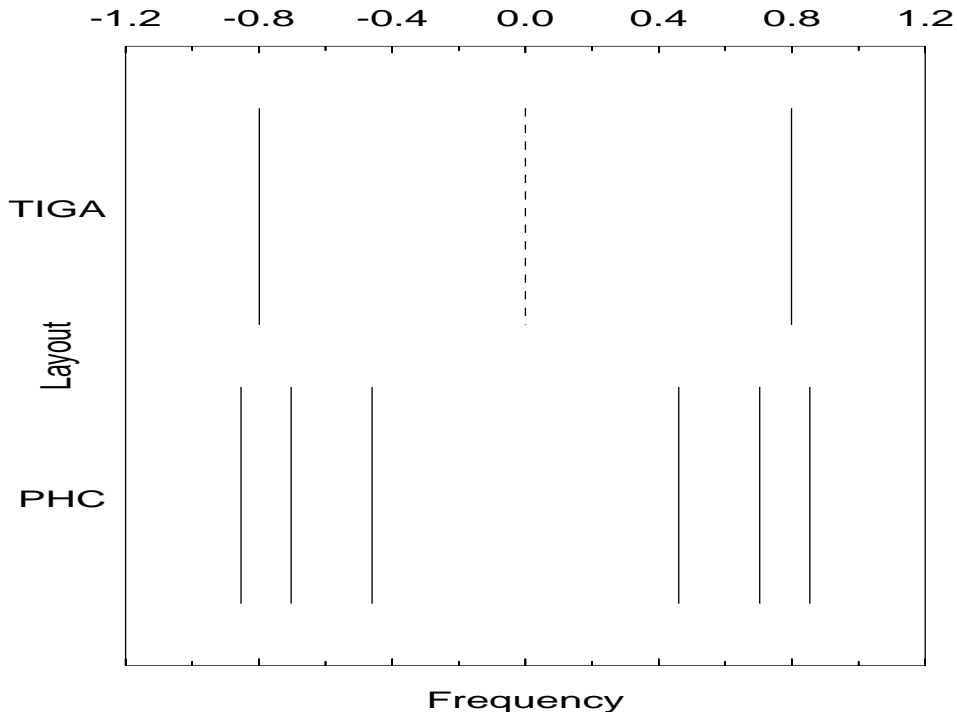


FIG. 6. Compared line spectrum of a coupled *TIGA* and a *PHC* resonator layout in an ideally spherical system. The weakly coupled central frequency in the *TIGA* is drawn dashed. The frequency pair is 5-fold degenerate for this layout, while the two outer pairs of the *PHC* are doubly degenerate each, and the inner pair is non-degenerate. Units in abscissas are $\eta^{1/2}\Omega$, and the central value, labeled 0.0, corresponds to Ω .

when the system is tuned to the nl -th spheroidal harmonic, i.e., $\Omega = \omega_{nl}$. It is immediately seen from here that the system response to this signal when the resonators are tuned to a monopole frequency is given by

$$\hat{q}_a(s) = \eta^{-1/2} (-1)^{J-1} \frac{f_0}{\sqrt{4\pi J}} |A_{n0}(R)| \frac{1}{2} \left[(s^2 + \omega_+^2)^{-1} - (s^2 + \omega_-^2)^{-1} \right], \quad \Omega = \omega_{n0} \quad (7.3)$$

an expression which holds for all a , and is independent of either the resonator layout or the hit point, which in particular prevents any determination of the latter, as obviously expected. The frequencies ω_{\pm} are those of (6.12), and we find here again a global factor $J^{-1/2}$, as also expected.

We consider next the situation when quadrupole tuning is implemented, $\Omega = \omega_{n2}$. We shall however do so only for the *TIGA* and *PHC* configurations, as more general considerations are not quite as interesting at this point.

A. *TIGA* response to a hammer stroke

One easily verifies that, for the TI configuration,

$$\hat{q}_a(s) = -\eta^{-1/2} \frac{5}{\sqrt{24\pi}} f_0 |A_{n2}(R)| \frac{1}{2} \left[(s^2 + \omega_+^2)^{-1} - (s^2 + \omega_-^2)^{-1} \right] P_2(\mathbf{n}_a \cdot \mathbf{n}_0), \quad \textit{TIGA} \quad (7.4)$$

where ω_{\pm} are the *TIGA* frequencies (6.20), and $\Omega = \omega_{n2}$. This equation shows that the hitting point position \mathbf{n}_0 can be easily determined from the readouts $\hat{q}_a(s)$ —as a matter of fact it is *redundantly* determined by them. The *mode channels* for this signal yield

$$\hat{y}^{(m)}(s) = -\eta^{-1/2} f_0 |A_{n2}(R)| \frac{1}{2} \left[(s^2 + \omega_+^2)^{-1} - (s^2 + \omega_-^2)^{-1} \right] Y_{2m}^*(\mathbf{n}_0), \quad m = -2, \dots, 2 \quad (7.5)$$

and they are proportional to the sphere's quadrupole radial oscillation amplitude $A_{n2}(R) Y_{2m}^*(\mathbf{n}_0)$ at the hit point, \mathbf{n}_0 [10]. A simple numerical simulation is illustrative of the situation, and we present it here.

We recall that the inverse Laplace transform of $2^{-1}[(s^2 + \omega_+^2)^{-1} - (s^2 + \omega_-^2)^{-1}]$ is

$$\Omega^{-1} \sin \frac{1}{2}(\omega_+ - \omega_-)t \cos \Omega t + O(\eta^{1/2}) \quad (7.6)$$

which is a *beat* —a sinusoid of carrier frequency Ω amplitude modulated by another sinusoid of much smaller frequency of order $\eta^{1/2}\Omega$. All six resonators' motions are thus identical beats, except that amplitude varies from one to the other, and the same applies to all five mode channels. We see this graphically in Figure 7, wherein plots are displayed of the resonator readouts and mode channels.

B. PHC response to a hammer stroke

The situation is slightly more involved for a *PHC* distribution, but still easy to address; the system response is given by

$$\hat{q}_a(s) = \eta^{-1/2} f_0 \sqrt{\frac{4\pi}{5}} |A_{n2}(R)| \sum_{m=-2}^2 \frac{1}{2} [(s^2 + \omega_{m+}^2)^{-1} - (s^2 + \omega_{m-}^2)^{-1}] \zeta_m^{-1} Y_{2m}(\mathbf{n}_a) Y_{2m}^*(\mathbf{n}_0), \quad \text{PHC} \quad (7.7)$$

and the mode channels by

$$\hat{y}^{(m)}(s) = \eta^{-1/2} f_0 |A_{n2}(R)| \frac{1}{2} [(s^2 + \omega_{m+}^2)^{-1} - (s^2 + \omega_{m-}^2)^{-1}] Y_{2m}^*(\mathbf{n}_0), \quad m = -2, \dots, 2 \quad (7.8)$$

The difference with the *TIGA* is this: the system response $q_a(t)$ is a *superposition of three different beats*, while the mode channels are *single beats* each, but with *differing modulation frequencies*. This is represented graphically in Figure 8, where we see the result of a numerical simulation of the *PHC* response to a hammer stroke, delivered to the solid at the same location as in the *TIGA* example of the previous subsection. The readouts $q_a(t)$ are somewhat fancy time series, whose frequency spectrum shows *three pairs of peaks* —in fact, the *lines* in the ideal spectrum of Figure 6. The mode channels on the other hand are *pure beats*, whose spectra consist of the *individually separate* pairs of previous peaks. It might perhaps be said that the *PHC* gives rise to a sort of “Zeeman splitting” of the *TIGA* degenerate frequencies, which can be attributed to an *axial symmetry breaking* of the isotropic character of that resonator distribution; the *PHC* mode channels naturally resolve the split multiplet into its components.

This simple example very neatly displays the most relevant features of both *TIGA* and *PHC* resonator distributions, and enables a quite clear comparison of the merits of either, which does apply also to real GW signals. Despite their distinct characteristics, these layouts are perfectly equivalent as regards their ability to sense GWs *in an ideally noiseless* detector. This is so simply because the detector is the sphere, not the transducers, and therefore *any* motion sensing system, not just these two, is equivalent to them if perfectly noiseless monitoring were possible. Things do however change in the presence of noise. T. Stevenson has recently addressed the problem of how isotropy in sensitivity is affected by noise [34], and concludes that while the *TIGA* maintains isotropic sensitivity, the *PHC* does not: the latter is slightly more sensitive in a relatively small solid angle around the resonators' axis, but slightly less for other incidence directions. This is a clear disadvantage of the *PHC*, but one may not forget that a real antenna will *not* be spherically symmetric because it must be *suspended*, and that breaks that symmetry. As we shall shortly see, the *PHC* is very naturally adapted to that symmetry breaking, and therefore it is probably unwise to outrightly dispose of it on the basis of a single noise criterion. At the same time, the *PHC* system spectrum is richer, and slightly broader than the *TIGA*'s, and this again favours *PHC*, even in the presence of noise, as the possibility of looking for signals at more frequencies reduces the probability of random disturbances, thereby increasing the probability of signal detection.

The above is a *qualitative* discussion, whose *quantitative* aspects will not be addressed in any more depth in this paper. We still wish to assess the effects of imperfections in a noiseless detector, which are of paramount relevance in a real system.

VIII. SYMMETRY DEFECTS

So far we have made the assumption that the sphere is perfectly symmetric, that the resonators are identical, that their locations on the sphere's surface are ideally accurate, etc. This is of course unrealistic. So we propose to address

now how such departures from ideality affect the system behaviour. As we shall see, the system is rather *robust*, in a sense to be made precise shortly, against a number of small defects.

In order to *quantitatively* assess ideality failures we shall adopt a philosophy which is naturally suggested by the results already obtained in an ideal system. It is as follows.

As we have seen in previous sections, the solution to the general equations (3.15) must be given as a *perturbative* series expansion in ascending powers of the small quantity $\eta^{1/2}$. This is clearly not a fact related to the system's symmetries, and so it will survive symmetry breakings. It is therefore appropriate to *parametrise* deviations from ideality in terms of suitable powers of $\eta^{1/2}$, in order to address them *consistently with the order of accuracy of the series solution to the equations of motion*. An example will better illustrate the situation.

In a *perfectly ideal* spherical detector the system frequencies are given by equations (5.4). Now, if a small departure from e.g. spherical symmetry is present in the system then we expect that a correspondingly small correction to those equations will be required. Which specific correction to the formula will actually happen can be *qualitatively* assessed by a *consistency* argument: if symmetry defects are of order $\eta^{1/2}$ then equations (5.4) will be significantly altered in their $\eta^{1/2}$ terms; if on the other hand such defects are of order η or smaller then any modifications to equations (5.4) will be swallowed into the $O(0)$ terms, and the more important $\eta^{1/2}$ terms will remain unaffected by this symmetry failure. We will say in the latter case that the system is *robust* to that ideality breaking.

More generally, this argument can be extended to see that the only system defects standing a chance to have any influences on lowest order ideal system behaviour are defects of order $\eta^{1/2}$ relative to an ideal configuration. Defects of such order are however *not necessarily guaranteed* to be significant, and a specific analysis is required for each specific parameter in order to see whether or not the system response is *robust* against the considered parameter deviations.

We therefore proceed as follows. Let P be one of the system parameters, e.g. a sphere frequency, or a resonator mass or location, etc. Let P_{ideal} be the *numerical value* this parameter has in an ideal detector, and let P_{real} be its value in the real case. These two will be assumed to differ by terms of order $\eta^{1/2}$, or

$$P_{\text{real}} = P_{\text{ideal}} (1 + p \eta^{1/2}) \quad (8.1)$$

For a given system, p is readily determined adopting (8.1) as the *definition* of P_{real} , once a suitable *hypothesis* has been made as to which is the value of P_{ideal} . In order for the following procedure to make sensible sense it is clearly required that p be of order 1 or, at least, appreciably larger than $\eta^{1/2}$. Should p thus calculated from (8.1) happen to be too small, i.e., of order $\eta^{1/2}$ itself or smaller, then the system will be considered *robust* as regards the affected parameter.

We now apply this criterion to various departures from ideality.

A. The suspended sphere

An earth based observatory obviously requires a *suspension mechanism* for the large sphere. If a *nodal point* suspension is e.g. selected then a diametral *bore* has to be drilled across the sphere [21]. The most immediate consequence of this is that spherical symmetry is broken, what in turn results in *degeneracy lifting* of the free spectral frequencies ω_{nl} , which now *split* up into multiplets ω_{nlm} ($m = -l, \dots, l$). The resonators' frequency Ω *cannot* therefore be matched to *the* frequency $\omega_{n_0 l_0}$, but at most to *one* of the $\omega_{n_0 l_0 m}$'s. In this subsection we keep the hypothesis that all the resonators are identical—we shall relax it later—and assume that Ω falls *within* the span of the multiplet of the $\omega_{n_0 l_0 m}$'s. Then we write

$$\omega_{n_0 l_0 m}^2 = \Omega^2 (1 + p_m \eta^{1/2}), \quad m = -l_0, \dots, l_0 \quad (8.2)$$

We now search for the coupled frequencies, i.e., the roots of equation (3.18). The kernel matrix $\hat{K}_{ab}(s)$ is however no longer given by (4.2), due the removed degeneracy of ω_{nl} , and we must stick to its general expression (3.17), or

$$\hat{K}_{ab}(s) = \sum_{nlm} \frac{\Omega_b^2}{s^2 + \omega_{nlm}^2} |A_{nl}(R)|^2 \frac{2l+1}{4\pi} Y_{lm}^*(\mathbf{n}_a) Y_{lm}(\mathbf{n}_b) \equiv \sum_{nlm} \frac{\Omega_b^2}{s^2 + \omega_{nlm}^2} \chi_{ab}^{(nlm)} \quad (8.3)$$

Following the steps of section 4 we now need to seek the roots of the equation

$$\det \left[\delta_{ab} + \eta \sum_{m=-l_0}^{l_0} \frac{\Omega^2 s^2}{(s^2 + \Omega^2)(s^2 + \omega_{n_0 l_0 m}^2)} \chi_{ab}^{(n_0 l_0 m)} + \eta \sum_{nl \neq n_0 l_0, m} \frac{\Omega^2 s^2}{(s^2 + \Omega^2)(s^2 + \omega_{nlm}^2)} \chi_{ab}^{(nlm)} \right] = 0 \quad (8.4)$$

Since Ω relates to $\omega_{n_0 l_0 m}$ through equation (8.2) we see that the roots of (8.4) follow again into either of the two categories (5.2), i.e., roots close to $\pm i\Omega$ and roots close to $\pm i\omega_{nlm}$ ($nl \neq n_0 l_0$). We shall exclusively concentrate on the former now. Direct substitution of the series (5.2a) into (8.4) yields the following equation for the coefficient $\chi_{\frac{1}{2}}$:

$$\det \left[\delta_{ab} - \frac{1}{\chi_{\frac{1}{2}}} \sum_{m=-l_0}^{l_0} \frac{\chi_{ab}^{(n_0 l_0 m)}}{\chi_{\frac{1}{2}} - p_m} \right] = 0 \quad (8.5)$$

This is a variation of (5.3), to which it reduces when $p_m = 0$, i.e., when there is full degeneracy.

The solutions to (8.5) no longer come in symmetric pairs, like (5.4). Rather, there are $2l_0+1+J$ of them, with a *maximum* number of $2(2l_0+1)$ non-identically zero roots if $J \geq 2l_0+1$ ¹⁰. For example, if we choose to select the resonators' frequency close to a quadrupole multiplet ($l_0=2$) then (8.5) has at most $5+J$ non-null roots, *with a maximum ten* no matter how many resonators in excess of 5 we attach to the sphere. Modes associated to null roots of (8.5) can be seen to be *weakly coupled*, just like in a free sphere, i.e., their amplitudes are smaller than those of the strongly coupled ones by factors of order $\eta^{1/2}$.

In order to assess the reliability of this method we have applied it to see what are its predictions for a *real system*. To this end, data taken with the *TIGA* prototype at *LSU*¹¹ were used to confront with. The *TIGA* was drilled and suspended from its centre, so its first quadrupole frequency split up into a multiplet of five frequencies. Their reportedly measured values are

$$\omega_{120} = 3249 \text{ Hz} , \quad \omega_{121} = 3238 \text{ Hz} , \quad \omega_{12-1} = 3236 \text{ Hz} , \quad \omega_{122} = 3224 \text{ Hz} , \quad \omega_{12-2} = 3223 \text{ Hz} , \quad (8.6)$$

All 6 resonators were equal, and had the following characteristic frequency and mass, respectively:

$$\Omega = 3241 \text{ Hz} , \quad \eta = \frac{1}{1762.45} \quad (8.7)$$

Substituting these values into (8.2) it is seen that

$$p_0 = 0.2075 , \quad p_1 = -0.0777 , \quad p_{-1} = -0.1036 , \quad p_2 = -0.4393 , \quad p_{-2} = -0.4650 \quad (8.8)$$

Equation (8.5) can now be readily solved once the resonator positions are fed into the matrices $\chi_{ab}^{(12m)}$. Such positions correspond to the pentagonal faces of a truncated icosahedron. Merkwitz [21] gives a complete account of all the measured system frequencies as resonators are progressively attached to the selected faces, beginning with one and ending with six. In Figure 9 we present a graphical display of the experimentally reported frequencies along with those calculated theoretically by solving equation (8.5). In Table 1 we give the numerical values. As can be seen, coincidence between our theoretical predictions and the experimental data is remarkable: the worst error is 0.2%, while for the most part it is below 0.1%. This should be taken as very strong evidence that our theoretical model *is* correct, since *discrepancies between its predictions and experiment are of order η* , as indeed expected —see (8.7). In addition, it is also reported in reference [22] that the 11-th, weakly coupled mode of the *TIGA* (highlighted in square brackets in Table I) has a practically zero amplitude, again in excellent agreement with our general theoretical predictions about modes beyond the tenth —see paragraph after equation (8.5).

This is an encouraging result which motivated us to try a better fit by estimating the *next order* corrections, i.e., χ_1 of (5.2a). As it turned out, however, matching between theory and experiment did not consistently improve. This is not really that surprising, though, as M&J explicitly state [22] that control of the general experimental conditions in which data were obtained had a certain degree of tolerance, and they actually show satisfaction that $\sim 1\%$ coincidence between theory and measurement is comfortably accomplished. But 1% is *two orders of magnitude larger than η* —cf. equation (8.7)—, so failure to refine our frequency estimates to order η is fully consistent with the accuracy of available real data.

We do expect that the analytical procedures developed in this paper will be the appropriate ones to assess and theoretically understand the system behaviour as rigor in system parameter control is progressively gained.

¹⁰ This is a *mathematical fact*, whose proof is relatively cumbersome, and will be omitted here; we just mention that it has its origin in the linear dependence of more than $2l_0+1$ spherical harmonics of order l_0 .

¹¹ These data are contained in reference [21], and we want to express our gratitude to Stephen Merkwitz for kindly handing them to us.

TABLE I. Numerical values of measured and theoretically predicted frequencies (in Hz) for the *TIGA* prototype with varying number of resonators. Percent differences are also shown. The *calculated* values of the tuning and free multiplet frequencies are taken *by definition* equal to the measured ones, and quoted in brackets. In square brackets the frequency of the *weakly coupled* sixth mode in the full, 6 resonator *TIGA* layout. These data are plotted in Figure 9.

| Item | Measured (Hz) | Calculated (Hz) | % difference | Item | Measured (Hz) | Calculated (Hz) | % difference |
|----------------|---------------|-----------------|--------------|--------------|---------------|-----------------|--------------|
| Tuning | 3241 | (3241) | (0.00) | 4 resonators | 3159 | 3155 | -0.12 |
| Free multiplet | 3223 | (3223) | (0.00) | | 3160 | 3156 | -0.11 |
| | 3224 | (3224) | (0.00) | | 3168 | 3165 | -0.12 |
| | 3236 | (3236) | (0.00) | | 3199 | 3198 | -0.05 |
| | 3238 | (3238) | (0.00) | 3236 | 3236 | 0.00 | |
| | 3249 | (3249) | (0.00) | 3285 | 3286 | 0.03 | |
| 1 resonator | 3167 | 3164 | -0.08 | 3310 | 3310 | 0.00 | |
| | 3223 | 3223 | 0.00 | 3311 | 3311 | 0.00 | |
| | 3236 | 3235 | -0.02 | 3319 | 3319 | 0.00 | |
| | 3238 | 3237 | -0.02 | 5 resonators | 3152 | 3154 | 0.08 |
| | 3245 | 3245 | 0.00 | | 3160 | 3156 | -0.14 |
| 2 resonators | 3305 | 3307 | 0.06 | | 3163 | 3162 | -0.03 |
| | 3160 | 3156 | -0.13 | | 3169 | 3167 | -0.08 |
| | 3177 | 3175 | -0.07 | | 3209 | 3208 | -0.02 |
| | 3233 | 3233 | 0.00 | | 3268 | 3271 | 0.10 |
| | 3236 | 3236 | 0.00 | 3304 | 3310 | 0.17 | |
| 3 resonators | 3240 | 3240 | 0.00 | 3310 | 3311 | 0.03 | |
| | 3302 | 3303 | 0.03 | 3313 | 3316 | 0.10 | |
| | 3311 | 3311 | 0.00 | 3319 | 3321 | 0.06 | |
| | 6 resonators | 3160 | 3155 | -0.15 | 3151 | 3154 | 0.11 |
| | | 3160 | 3156 | -0.13 | 3156 | 3155 | -0.03 |
| | | 3191 | 3190 | -0.02 | 3162 | 3162 | 0.00 |
| | | 3236 | 3235 | -0.02 | 3167 | 3162 | -0.14 |
| | | 3236 | 3236 | 0.00 | 3170 | 3168 | -0.07 |
| | | 3297 | 3299 | 0.08 | [3239] | [3241] | [0.06] |
| | | 3310 | 3311 | 0.02 | 3302 | 3309 | 0.23 |
| 3311 | | 3311 | 0.00 | 3308 | 3310 | 0.06 | |
| | | | | 3312 | 3316 | 0.12 | |
| | | | | 3316 | 3317 | 0.02 | |
| | | | 3319 | 3322 | 0.10 | | |

A final word on a technical issue is in order. Merkwitz and Johnson's equations for the *TIGA* [19,20] are identical to ours to lowest order in η . Remarkably, though, their reported theoretical estimates of the system frequencies are not quite as accurate as ours. The reason for this is probably the following: in M&J's model these frequencies appear within an algebraic system of $5+J$ linear equations with as many unknowns which has to be solved; in our model the algebraic system has only J equations and unknowns, actually equations (3.15). This is a very appreciable difference indeed for the range of values of J under consideration. While the roots for the frequencies can be seen to *mathematically* coincide in both approaches, in actual practice these roots are *estimated*, generally by means of computer programmes. It is here that problems most likely arise, for the numerical reliability of an algorithm to solve matrix equations normally decreases as the rank of the matrix increases. The significant algebraic simplification of our model's equations should therefore be considered one of real practical value.

1. The suspended PHC

We briefly consider now which would be the effects of symmetry breaking due to suspension in a *PHC* resonator distribution. The natural suspension axis is the symmetry axis of the resonators, so we shall assume that 5 of them are attached to the detector around that axis as described in the paragraphs before equation (6.30). To be specific, we shall speculate with a *PHC* having the numerical parameters of equations (8.6) and (8.7), a hypothetical but reasonable conjecture which will enable comparison with the actual *TIGA* prototype.

The results are displayed in Figure 10. It is at once apparent that the structure of the frequency pairs in a *drilled PHC* is quite similar to that of the perfect *PHC*, while the drilled *TIGA* pairs are qualitatively different from those

of the ideal *TIGA*. This is not particularly surprising given the symmetries of both layouts, and is an indication that axially symmetric distributions may be an interesting alternative to more symmetric distributions in a real system, as their geometry naturally adapts to the suspension device, and also require *fewer* transducers.

B. Other mismatched parameters

We finally devote a few words to assess the system sensitivity to small mismatches in resonators' masses, locations and frequencies.

1. Resonator mass mismatches

If the *masses* are slightly non-equal then we can write

$$M_a = \eta \mathcal{M} (1 + \mu_a \eta^{1/2}) , \quad a = 1, \dots, J \quad (8.9)$$

where η can be defined e.g. as the ratio of the *average* resonator mass to the sphere's mass. It is immediately obvious from equation (8.9) that mass non-uniformities of the resonators only affect our equations in *second order*, since resonator mass non-uniformities result, as we see, in corrections of order $\eta^{1/2}$ to $\eta^{1/2}$ itself, which is the very parameter of the perturbative expansions. The system is thus clearly *robust* to mismatches in the resonator masses of the type (8.9).

2. Errors in resonator locations

The same happens if the *locations* of the resonators have tolerances relative to a *pre-selected* distribution. For let \mathbf{n}_a be a set of resonator locations, for example the *TIGA* or the *PHC* positions, and let \mathbf{n}'_a be the real ones, close to the former:

$$\mathbf{n}'_a = \mathbf{n}_a (1 + \mathbf{v}_a \eta^{1/2}) , \quad a = 1, \dots, J \quad (8.10)$$

The values \mathbf{n}_a determine the eigenvalues ζ_a in equation (5.4), and also they appear as arguments to the spherical harmonics in the system response functions of sections 6 and 7. It follows from (8.10) by continuity arguments that

$$Y_{lm}(\mathbf{n}'_a) = Y_{lm}(\mathbf{n}_a) + O(\eta^{1/2}) \quad (8.11a)$$

$$\zeta'_a = \zeta_a + O(\eta^{1/2}) \quad (8.11b)$$

Inspection of the equations of sections 5–7 shows that both ζ_a and $Y_{lm}(\mathbf{n}_a)$ *always* appear within lowest order terms, and hence that corrections to them of the type (8.11) will affect those terms in *second order* again. We thus conclude that the system is also *robust* to small misalignments of the resonators relative to pre-established positions.

3. Resonator frequency mistunings

The resonator *frequencies* may also differ amongst them, so let

$$\Omega_a = \Omega (1 + \rho_a \eta^{1/2}) , \quad a = 1, \dots, J \quad (8.12)$$

To assess the consequences of this, however, we must go back to equation (3.18) and see what the coefficients in its series solutions of the type (5.2a) are. The procedure is very similar to that of section VIII A, and will not be repeated here; the lowest order coefficient $\chi_{\frac{1}{2}}$ is seen to satisfy the algebraic equation

$$\det \left[\delta_{ab} - \frac{1}{\chi_{\frac{1}{2}}} \sum_{c=0}^J \frac{\chi_{ac}^{(n_0 l_0)} \delta_{cb}}{\chi_{\frac{1}{2}} - \rho_c} \right] = 0 \quad (8.13)$$

which reduces to (5.3) when all the ρ 's vanish, as expected. This appears to potentially have significant effects on our results to lowest order in $\eta^{1/2}$, but a more careful consideration of the facts shows that it is probably unrealistic to

think of such large tolerances in resonator manufacturing as implied by equation (8.12) in the first place. In the *TIGA* experiment, for example [21], an error of order $\eta^{1/2}$ would amount to around 50 Hz of mistuning between resonators, an absurd figure by all means. In a full scale sphere (~ 40 tons, ~ 3 metres in diameter, ~ 800 Hz fundamental quadrupole frequency, $\eta \sim 10^{-5}$) the same error would amount to between 5 Hz and 10 Hz in resonator mistunings for the lowest frequency. This is probably excessive for a capacitive transducer, but may be realistic for an inductive one. With this exception, it is thus more appropriate to consider that resonator mistunings are at least of order η . If this is the case, though, we see once more that the system is quite insensitive to such mistunings.

Summing up the results of this section, we can say that the resonator system dynamics is quite *robust* to small (of order $\eta^{1/2}$) changes in its various parameters. The important exception is of course the effect of suspension drillings, which do result in significant changes relative to the ideally perfect device, but which can be relatively easily calculated. This theoretical picture is fully supported by experiment, as *robustness* in the parameters here considered has been reported in reference [22].

IX. CONCLUSIONS

A spherical GW antenna is a natural multimode device with very rich potential capabilities to detect GWs on earth. But such detector is not just a bare sphere, it requires a set of *motion sensors* to be practically useful. It appears that transducers of the *resonant* type are the best suited ones for an efficient performance of the detector. *Resonators* however significantly *interact* with the sphere, and they affect in particular its frequency spectrum and vibration modes in a specific fashion, which has to be properly understood before reliable conclusions can be drawn from the system readout.

The main objective of this paper has been the construction and development of an elaborate theoretical model to describe the joint dynamics of a solid elastic sphere and a set of *radial motion* resonators attached to its surface at arbitrary locations, with the purpose to make predictions of the system characteristics and response, in principle with arbitrary mathematical precision.

We have shown that the solutions to our equations of motion must necessarily be given as an ascending series in powers of the small “coupling constant” η , the ratio of the average resonator mass to the mass of the large sphere. The *lowest order* approximation corresponds to terms of order $\eta^{1/2}$ and, to this order, we recover, and widely generalise, other authors’ results [22,33,34], obtained by them on the basis of certain simplifying assumptions. This has in particular enabled us to assess the system response for arbitrary resonator layouts, and to search the equations for configurations other than the highly symmetric *TIGA*, whose properties and/or performance may thus be comparatively assessed. This search has led us to make a specific proposal, the *PHC*, which is based on a pentagonally symmetric set of 5 rather than 6 resonators per quadrupole mode sensed. This *PHC* distribution presents a somewhat wider frequency spectrum than the *TIGA*, and has the interesting property that different *wave amplitudes* selectively couple to different *detector modes* having different frequencies, so that the antenna’s mode channels come at different rather than equal frequencies. The *PHC* philosophy can be extended to make a *multifrequency* system by using resonators tuned to the first two quadrupole harmonics of the sphere *and* to the first monopole, an altogether 11 transducer set [23].

The assessment of *symmetry failure* effects, as well as other parameter departures from ideality, has also interested us here. This is seen to receive a particularly clear treatment in our general scheme: the theory transparently shows that the system is *robust* against relative disturbances of order η or smaller in any system parameters, and provides a systematic procedure to assess larger tolerances —up to order $\eta^{1/2}$. The system is shown to still be robust to tolerances of this order in some of its parameters, whilst it is not to others. Included in the latter group is the effect of spherical symmetry breaking due to system suspension in the laboratory, which causes *degeneracy lifting* of the sphere’s eigenfrequencies, now split up into multiplets. By using our algorithms we have succeeded in numerically *reproducing* the reportedly measured frequencies of the *LSU* prototype antenna with fully satisfactory precision. The experimentally reported robustness of the system to resonator mislocations [22] is also in full agreement with our theoretical predictions.

We take this numerical success as a strong indication that our model *is* correct. Beyond that, though, we also feel it sheds much light into the *principles* of the functioning of a spherical GW antenna with resonant transducers, as every result ultimately follows from very general and fundamental principles, i.e., equations (2.12). In addition, our master equations (3.15) are actually *simpler* than e.g. Merkowitz and Johnson’s [19,22], since they are fewer in number, yet they contain *more* information about the system, as they are accurate to arbitrary order in η . *Lowest order* solutions to these equations are thus already simpler, and this has an obvious *practical* value. But *higher order* corrections can, and must, be estimated by suitable analysis of those equations. We have not attempted to comprehensively discuss fine structure corrections in this paper, which will likely be necessary as experimental techniques improve. We defer

them to near future work.

ACKNOWLEDGMENTS

We are indebted with Stephen Merkwitz for his kind supply of the *TIGA* prototype data, without which a significant part of this work would have been speculative. Fruitful discussions with him are also gratefully acknowledged. We thank Eugenio Coccia for invaluable interaction and encouragement throughout the development of this research, and for the organisation of very interesting seminars in Rome to more openly discuss the topics of this paper. Thanks are also due to Curt Cutler for pointing out to us an initial error in equation (2.1b). We have received financial support from the Spanish Ministry of Education through contract number PB93-1050.

APPENDIX A:

We give in this Appendix a few important properties of the matrix $P_l(\mathbf{n}_a \cdot \mathbf{n}_b)$ for arbitrary l and resonator locations \mathbf{n}_a ($a=1, \dots, J$) which are useful for detailed system resonance characterisation.

We first note the *summation formula* for spherical harmonics [26]

$$\sum_{m=-l}^l Y_{lm}^*(\mathbf{n}_a) Y_{lm}(\mathbf{n}_b) = \frac{2l+1}{4\pi} P_l(\mathbf{n}_a \cdot \mathbf{n}_b), \quad a, b = 1, \dots, J \quad (\text{A1})$$

with an obvious change of notation in the arguments to the spherical harmonics, and where P_l is a Legendre polynomial:

$$P_l(z) = \frac{1}{2^l l!} \frac{d^l}{dz^l} (z^2 - 1)^l \quad (\text{A2})$$

To ease the notation we shall use the symbol \mathcal{P}_l to mean the entire $J \times J$ matrix $P_l(\mathbf{n}_a \cdot \mathbf{n}_b)$, and introduce Dirac *kets* $|m\rangle$ for the column J -vectors

$$|m\rangle \equiv \sqrt{\frac{4\pi}{2l+1}} \begin{pmatrix} Y_{lm}(\mathbf{n}_1) \\ \vdots \\ Y_{lm}(\mathbf{n}_J) \end{pmatrix}, \quad m = -l, \dots, l \quad (\text{A3})$$

These kets are *not* normalised; in terms of them equation (A1) can be rewritten in the more compact form

$$\mathcal{P}_l = \sum_{m=-l}^l |m\rangle \langle m| \quad (\text{A4})$$

Equation (A4) indicates that the *rank* of the matrix \mathcal{P}_l cannot exceed $(2l+1)$, as there are only $(2l+1)$ kets $|m\rangle$. So, if $J > (2l+1)$ then it has at least $(J-2l-1)$ identically null eigenvalues —there can be more if some of the \mathbf{n}_a 's are parallel, as this causes rows (or columns) of \mathcal{P}_l to be repeated.

We now prove that the non-null eigenvalues of \mathcal{P}_l are *positive*. Clearly, a regular eigenvector, $|\phi\rangle$, say, of \mathcal{P}_l will be a linear combination of the kets $|m\rangle$:

$$\mathcal{P}_l |\phi\rangle = \zeta^2 |\phi\rangle, \quad |\phi\rangle = \sum_{m=-l}^l \phi_m |m\rangle \quad (\text{A5})$$

where we have called ζ^2 the corresponding eigenvalue, since it is a positive number, as we shall shortly prove. If the second (A5) is substituted into the first then it is immediately seen that

$$\sum_{m'=-l}^l (\zeta^2 \delta_{mm'} - \langle m|m'\rangle) \phi_{m'} = 0 \quad (\text{A6})$$

which admits non-trivial solutions if and only if

$$\det (\zeta^2 \delta_{mm'} - \langle m|m' \rangle) = 0 \quad (\text{A7})$$

In other words, ζ^2 are the eigenvalues of the $(2l+1) \times (2l+1)$ matrix $\langle m|m' \rangle$, which is positive definite because so is the “scalar product” $\langle \phi|\phi' \rangle$. All of them are therefore strictly positive.

Finally, since the *trace* is an invariant property of a matrix, and

$$\text{trace}(\mathcal{P}_l) \equiv \sum_{a=1}^J P_l(\mathbf{n}_a \cdot \mathbf{n}_a) = \sum_{a=1}^J 1 = J \quad (\text{A8})$$

we see that the eigenvalues ζ_a^2 add up to J :

$$\text{trace}(\mathcal{P}_l) = \sum_{a=1}^J \zeta_a^2 \equiv \sum_{\zeta_a \neq 0} \zeta_a^2 = J \quad (\text{A9})$$

- [1] R. Forward, *Gen. Rel. and Grav.* **2**, 149 (1971).
- [2] E. Coccia, G.Pizzella, F.Ronga (eds.), *Gravitational Wave Experiments*, Proceedings of the First Edoardo Amaldi Conference, World Scientific, Singapore, 1995.
- [3] E. Coccia, in M. Francaviglia, G. Longhi, L. Lusanna, and E. Sorace (eds.), *General Relativity and Gravitation, Proceedings of the GR-14 Conference*, World Scientific, Singapore, 1997.
- [4] Ashby N. and Dreitlein J., *Phys. Rev.* **D12**, 336 (1975).
- [5] R.V. Wagoner and H.J. Paik in *Experimental Gravitation*, Proceedings of the Pavia International Symposium, Acad. Naz. dei Lincei (1977).
- [6] There are collaborations in USA, Brazil, Holland, and Italy.
- [7] E. Coccia, V. Fafone, G. Frossati, J.A. Lobo, J.A. Ortega, *The hollow sphere as a detector of GWs*, submitted to *Phys Rev D* (1997).
- [8] N.S. Magalhaes et al., *Mon. Not. R. Astron. Soc.* **274**, 670 (1995).
- [9] M. Brunetti, PhD Thesis, Roma (1997).
- [10] J.A. Lobo, *Phys. Rev.* **D52**, 591 (1995).
- [11] Bianchi M., Coccia E., Colacino C.N., Fafone V. and Fucito F. *Class. and Quantum Grav.* **13**, 2865 (1996).
- [12] Coccia E., Lobo J.A. and Ortega J.A., *Phys Rev D* **52**, 3735 (1995).
- [13] B.F. Schutz, in Gleiser R.J., Kozameh C.N. and Moreschi O.M., *General Relativity and Gravitation, Proceedings of the GR-13 Conference*, IOP, Bristol, UK (1993).
- [14] P. Rapagnani, *Nuovo Cimento* **5C**, 385 (1982).
- [15] J-P. Richard, *Phys. Rev. Lett.* **521**, 165 (1984).
- [16] H.J. Paik, in reference [2] above.
- [17] P. Astone *et al.*, *Phys. Rev.* **D47**, 2 (1993).
- [18] Astone P. *et al.*, *Europhys. Lett.* **16**, 231 (1991).
- [19] W. Johnson and S.M. Merkowitz, *Phys Rev Lett* **70**, 2367 (1993).
- [20] S.M. Merkowitz and W. Johnson, *Phys Rev D* **51**, 2546 (1995).
- [21] S.M. Merkowitz, *PhD Thesis*, Louisiana State University (1995).
- [22] S.M. Merkowitz and W. Johnson, to appear in the December-15-1997 issue of *Phys Rev D*.
- [23] J.A. Lobo and M.A. Serrano, *Europhys. Lett.* **35**, 253 (1996).
- [24] J.A. Lobo and M.A. Serrano, *Class. and Quantum Grav.* **14**, 1495 (1997).
- [25] Landau L.D. and Lifshitz E.M., *Theory of Elasticity*, Pergamon Press, Oxford (1970).
- [26] Edmonds A.R., *Angular Momentum in Quantum Mechanics*, Princeton Univ. Press 1960.
- [27] We use here the better adapted notation a_{n0} and a_{n2} instead of a_n and b_n , respectively, of reference [10]. Numerical values are however identical.
- [28] Brans C. and Dicke R. H., *Phys. Rev.* **124**, 925 (1961)
- [29] F.G. Tricomi, *Integral equations*, Interscience Publishers (1957).
- [30] D. Porter and D.S.G. Stirling, *Integral equations: a practical treatment, from spectral theory to applications*, Cambridge Univ. Press (1990).
- [31] C.W. Helstrom, *Statistical Theory of Signal Detection*, Pergamon Press, Oxford (1968).
- [32] B.H. Bransden and C.J. Joachain, *Physics of atoms and molecules*, Longman (1984).

- [33] N.S. Magalhães, O.D. Aguiar, W.W. Johnson and C. Frajuca, *GRG* **29**, 1509 (1997).
- [34] T.R. Stevenson, to appear in *Phys. Rev. D*, July 15 issue (1997).
- [35] Typically, such formulas contain higher order terms in η which are calculated on the assumption that only tuned modes couple to resonators. They are therefore in error by relative magnitudes of order $\eta^{1/2}$.
- [36] A. Holden, *Formes, espace et symétries*, CEDIC (1977).
- [37] Z. Har'El, *Geometriæ Dedicata* **47**, 57 (1993).
- [38] E. Coccia and V. Fafone, *Phys. Lett. A* **213**, 16 (1996).
- [39] A. Krolak, J.A. Lobo and B.J. Meers, *Phys. Rev. D* **43**, 2470 (1991).
- [40] A. Krolak, J.A. Lobo and B.J. Meers, *Phys. Rev. D* **47**, 2184 (1993).

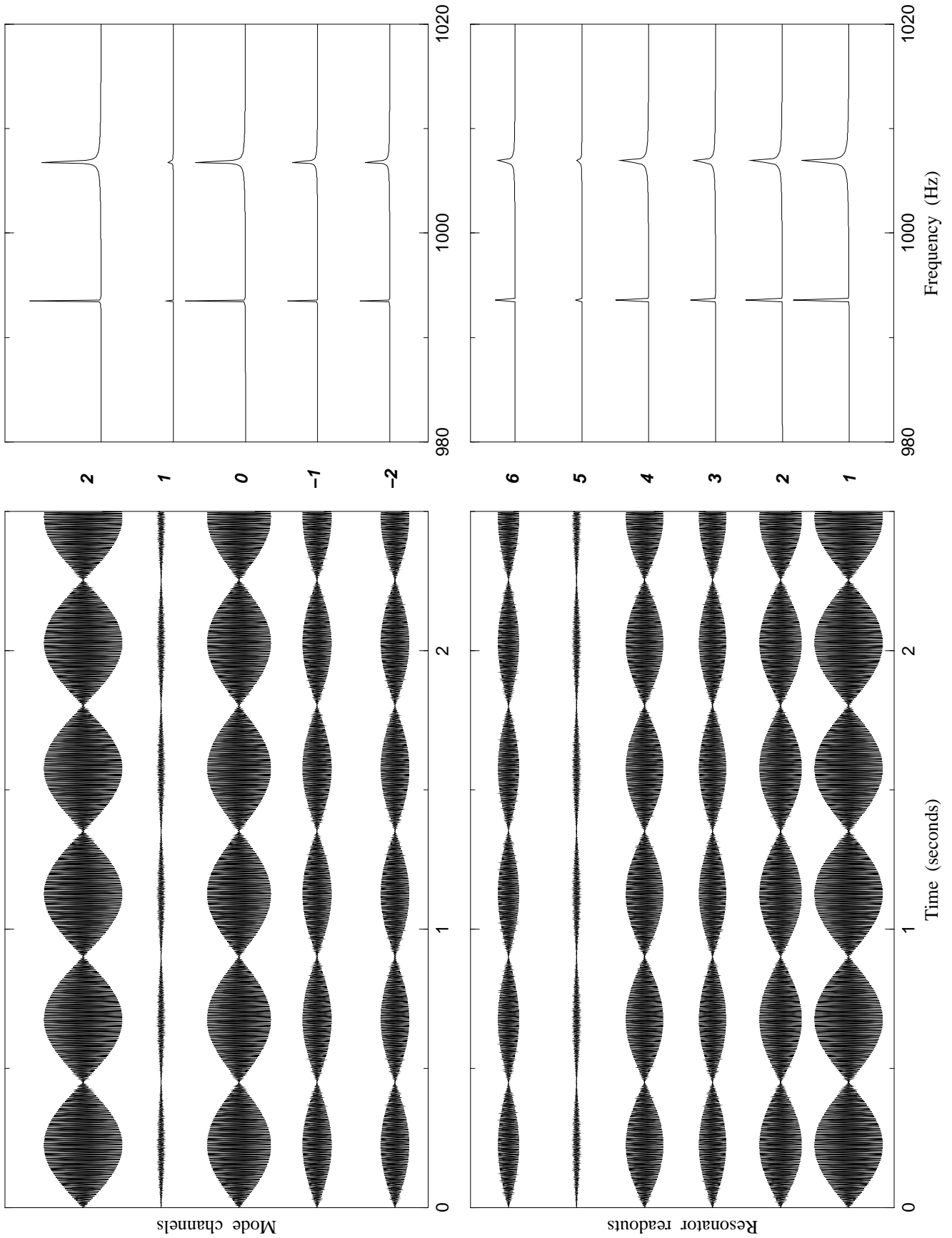


FIG. 7. Simulated response of a *TIGA* to a hammer stroke: the time series and their respective spectra, both for direct resonator readouts and mode channels. Asymmetric widening of spectral lines is due to frequency *leakage* caused by finite integration time.

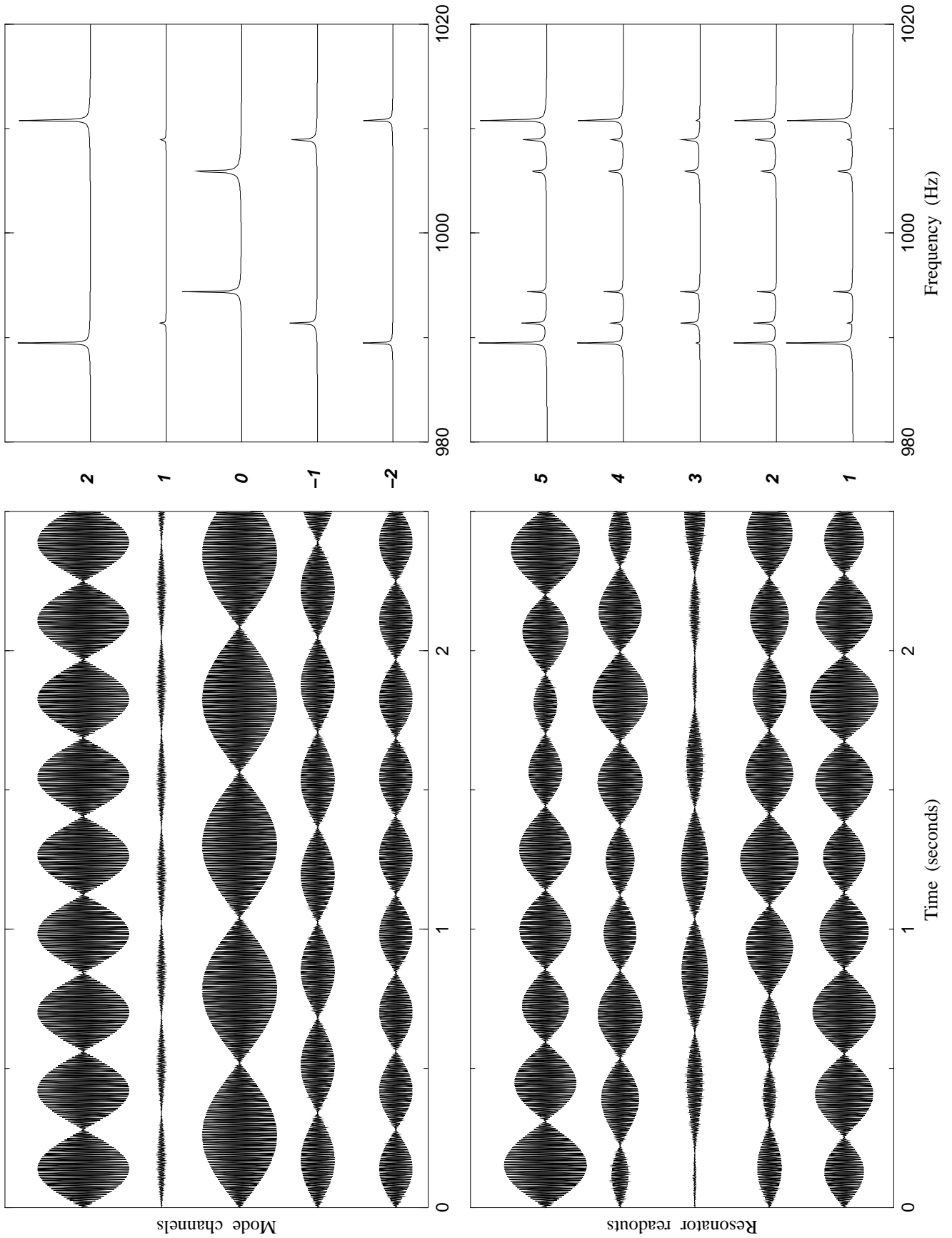


FIG. 8. Simulated response of a *PHC* to a hammer stroke: the time series and their respective spectra, both for direct resonator readouts and mode channels. Note that while the former are *not* simple beats, the latter are.

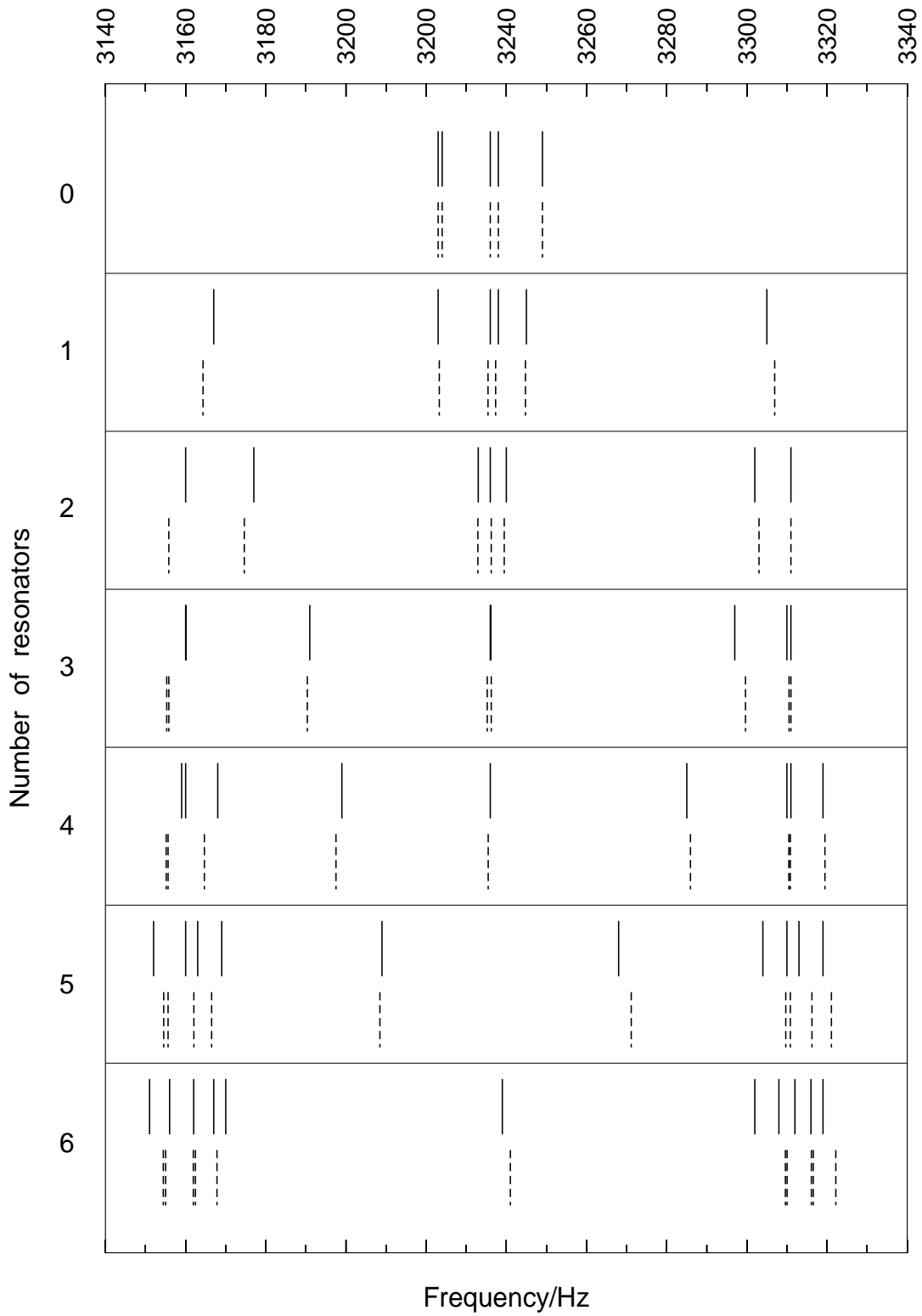


FIG. 9. The frequency spectrum of the *TIGA* distribution as resonators are progressively added from none to 6. Continuous lines correspond to measured values, and dashed lines correspond to their $\eta^{1/2}$ theoretical estimates of equation (8.5).

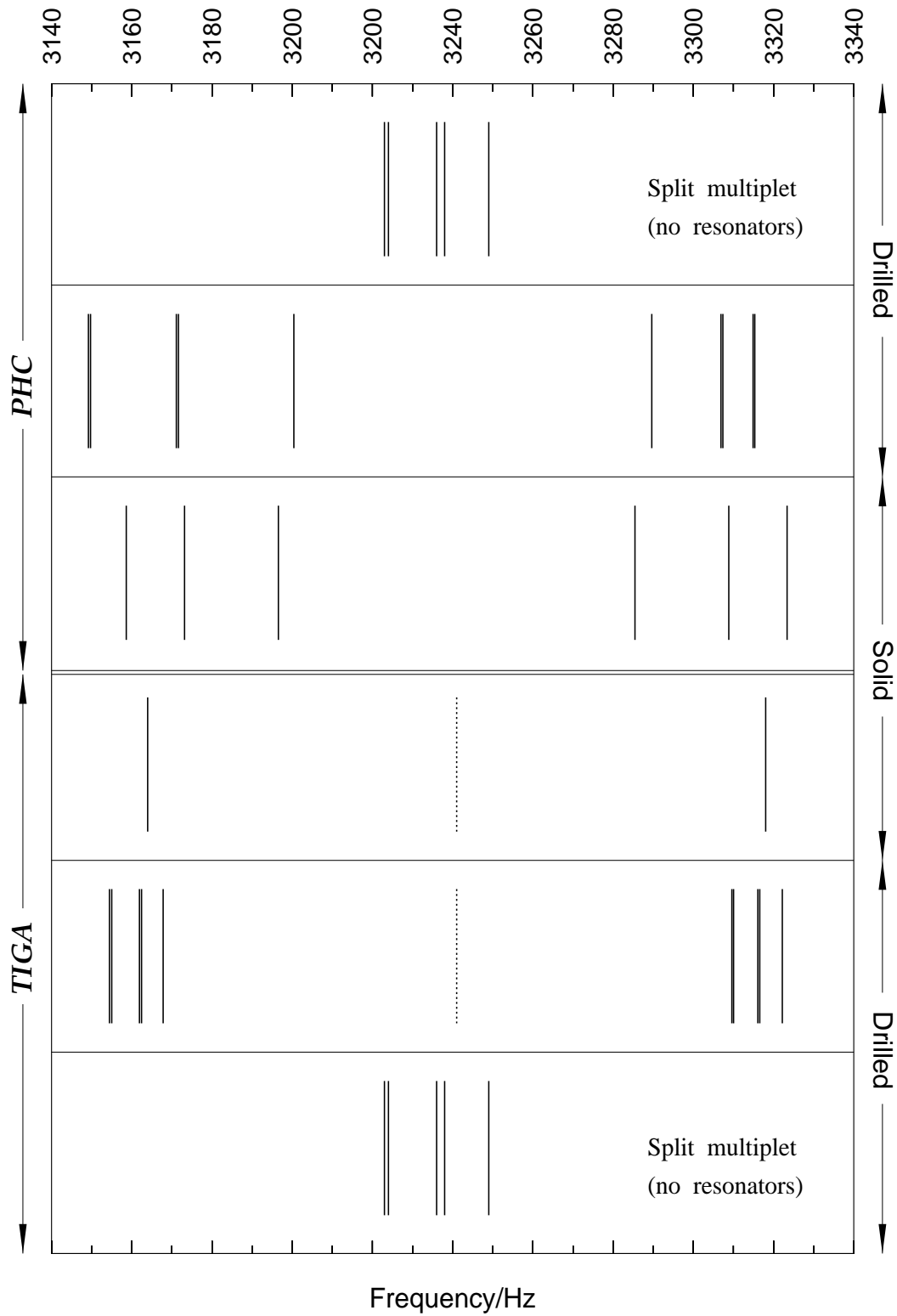


FIG. 10. A comparative display of the line spectra of a *TIGA* and a *PHC*, both in a hypothetically perfect solid shape (centre) and in a more realistic, drilled-for-suspension device (bottom and top, respectively). *TIGA* data are real, see Figure 9, while *PHC* data are speculative on the basis of reasonable assumptions —see text.